ABSTRACT

FORMULATION OF UV CURABLE RESINS UTILIZED IN VAT PHOTO POLYMERIZATION FOR THE ADDITIVE MANUFACTURING OF GUN PROPULSION CHARGE IN 3D PRINTERS

by
David T. Bird

Formulating resins for Additive Manufacturing (AM), utilizing UV laser stereolithography, is a new technique that makes it possible for the fabrication of complex geometries with high dimensional resolution. This layer by layer photopolymerization approach spans various industrial sectors from adhesives, inks and optical fibers to nanotechnology and biomaterials. UV curable resins such as epoxides, vinyl ethers and other acrylates are important monomers that offer effective mediums for energetic materials, and the potential exists to develop environmentally friendly formulations with suspended energetic materials at various solids loading levels.

Developing techniques for UV curing formulations of highly loaded energetic suspensions is a challenging feat that must satisfy several requirements and produce a high quality formulation with synergistic ingredient combinations to enhance propulsion phenomena. The candidate formulation must be able to operate in a SteroLithography Apparatus (SLA) resin tank, meaning the suspension must be at least as fluidic as conventional SLA resins; and a thorough understanding of the polymer network structure and cure kinetics is essential for a resulting polymer that exhibits good mechanical properties.

FORMULATION OF UV CURABLE RESINS UTILIZED IN VAT PHOTO POLYMERIZATION FOR THE ADDITIVE MANUFACTURING OF GUN PROPULSION CHARGE IN 3D PRINTERS

by
David T. Bird

A Thesis
Submitted to the Faculty of
New Jersey Institute of Technology
in Partial Fulfillment of the Requirements for the Degree of
Master of Science in Materials Science and Engineering

Interdisciplinary Program in Materials Science and Engineering

December 2017

Blank Page

FORMULATION OF UV CURABLE RESINS UTILIZED IN VAT PHOTO POLYMERIZATION FOR THE ADDITIVE MANUFACTURING OF GUN PROPULSION CHARGE IN 3D PRINTERS

David T. Bird

Dr. N.M. Ravindra, Thesis Advisor   Date
Professor of Physics, NJIT

Dr. Oktay Gokce, Committee Member   Date
Senior University Lecturer of Physics, NJIT

Dr. Murat Guvendiren, Committee Member   Date
Assistant Professor of Chemical, Biological and Pharmaceutical Engineering, NJIT

BIOGRAPHICAL SKETCH

Author: David T. Bird

Degree: Master of Science

Date: December 2017

Undergraduate and Graduate Education:

- Master of Science in Materials Science and Engineering,
  New Jersey Institute of Technology, Newark, NJ, 2018

- Bachelor of Science in Chemistry,
  Aston University, Birmingham, UK, 2009

Major: Materials Science and Engineering

Presentations and Publications:

David Bird, "Formulation of UV Curable Resins Utilized in Vat Photo Polymerization for the Additive Manufacturing of Gun Propulsion Charge in 3d Printers," The Sixty Fourth JANNAF Propulsion Meeting, Kansas City, USA, May 2017.

David Bird, Timothy M. Martin and Laibin B. Yan. "Foam Formulations and Emulsifiable Concentrates," Patent Application EP3160226 A1.3 May 2017.

To Mom and Dad
All the work and dedication are because you said I could do it.

ACKNOWLEDGMENT

TABLE OF CONTENTS

LIST OF TABLES

LIST OF FIGURES

CHAPTER I

INTRODUCTION

1.1 Motivation and Objective

The development of a photocurable suspension formulation for StereoLithography Apparatus (SLA) is a complex system that involves careful selection of resins and a thorough understanding of not only how the continuous monomer phase behaves with the discontinuous dispersed phase within, but how the resulting polymer impregnated with said solids behaves from the perspective of mechanical properties after photopolymerization.

The photopolymerization development connected with SLA, in this study, utilizes a resin tank that is optically transparent and filled with a liquid polymerizable material. Irradiating the build region from underneath the transparent resin tank containing the unpolymerized material will result in a solid thin layer of the liquid polymerizable material in a "bottom up" approach to constructing a three-dimensional object. Ultraviolet (UV) light is the irradiation source used for developing the solid polymer in a layer-by-layer formation; and essential to formation of the polymer is the incorporation of a photoinitiator (PI) that absorbs UV energy in the spectral area that the UV energy source emits [1]. Of further importance is the efficiency of the irradiation source as the energy delivered to the surface per unit area is inversely proportional to exposure (number of passes, duration) [2]. This work utilizes a commercial off-the-shelf (COTS) SLA 3D printer for forming complex geometries that are currently not able to be manufactured utilizing conventional processes.

The photopolymerization reaction that will be occurring within a formulation resin suspension will have competing factors such as solids inhibiting depth of cure and the limits of the printer. Therefore, photoinitiator concentration, solids loading, monomer

properties and structure, stability of the uncured formulation, and resulting mechanical properties of cured polymer are critical parameters to study for understanding the design space of SLA formulations; hence figuring out how to optimize mechanical properties based on this data is the main objective of this study.

1.2 Background Information ARDEC

The Propulsion Research and Engineering Branch of the U.S. Army Armament Research, Development and Engineering Center (ARDEC), in conjunction with its sister Army laboratories, other DoD partners and defense contractors have been exploring Additive Manufacturing (AM), and specifically SLA for the purpose of this work, as a method to investigate propulsion charges. Previously, formulation efforts of layering propellants by Manning, Park and Klingaman [3] were developed and utilized a high energy, high density energetic thermoplastic elastomer (ETPE) propellant for a solventless process in order to achieve progressive burning relative to pressure generation. The advantages of co-layered propellant translated to increased muzzle velocity without over pressurization within the gun. However, even though this was a successful method of maximizing the performance, the approaches were limited by manufacturing techniques and repeatability; which further yielded inferior quality that directly affected these higher performance charges. AM and 3D printed propulsion charges are predicted to innovate the layering and production of complex geometries that previous manufacturing techniques were not able to deliver [4].

Polymer nanocomposites have been a focus for propellant and explosive formulators with the goal to increase performance and modify the reactivity of energetic materials and their related systems [5]. The potential for its incorporation into the 3D printing world would capitalize on the performance enhancements including improved burn rates, easy ignition, higher specific impulse, improved combustion efficiency and a

greater potential for tuning performance through particle loading and size control. Synthesis techniques for polymer nanocomposites are characterized as either top-down or bottom-up. The top down approach (which is investigated in this paper) involves breaking down bulk materials gradually into smaller sizes and stabilizing the formulation against surface energy related phenomena such as aggregation and Ostwald Ripening. Examples of top-down processing include high-energy ball milling (investigated in this work), cryochemical processing, and combustion synthesis. Bottom-up methods, such as template synthesis, chemical (reactive) precipitation, and chemical vapor deposition rely on precursors to construct and grow well organized structures at the nanomeric level. Both methods have the potential to incorporate nanoparticles into 3D printable binders that can be used in conventional propellant production or conventional 3D printers.

CHAPTER 2

PHOTOPOLYMERIZATION AND MECHANICAL ANALYSES

2.1 Environmental Considerations and Health and Safety

The photopolymerization world is putting a high demand on performance in a period where sustainability, cost, environment, safety and health aspects are of great importance [1,5]. Toxicity associated with inhalation and ingestion is not concerning with UV materials, but skin exposure is important as these compounds are less volatile. Requirements such as low volatile organic compounds (VOC) and solvent free systems are becoming more of a necessity, thereby establishing photopolymerization as an ecological alternative to thermal systems through the reduction of VOCs. UV lamps do present an area of concern for skin and eyes, but with appropriate personal protective equipment (PPE), the hazard remains low. In addition to VOC free and solventless systems, biopolymers and biomaterials are getting significant attention because of environmental concerns and the movement away from petroleum based chemicals. In the present study, new syntheses and derivations concerning photopolymerization monomers and additives will be discussed.

A lot of work has focused on using water-soluble ingredients as it eliminates the use of organic solvents (normally incorporated to dissolve insoluble initiators), but this enhances the chances of soil mobility so many of the requirements remain difficult to achieve. Recently, Ritter et al [6] formulated a nearly water insoluble PI (2-hydroxy-2-methyl-1-phenylpropan-1-one) with β-Cyclodextrin to generate a water soluble PI. The resulting cyclodextrin/PI complex did also register a higher polymerization rate and better polymerization yield than the standalone α-hydroxy ketone in a kinetic study of

polymerization on *N*-isopropylacrylamide. In, general, cyclic oligosaccharides exhibit a torus-shaped structure with a hydrophobic cavity and hydrophilic exterior. These molecules are able to encapsulate hydrophobic PIs or their side groups within an aqueous solution or in an emulsion [7]. See Figure 2.1.
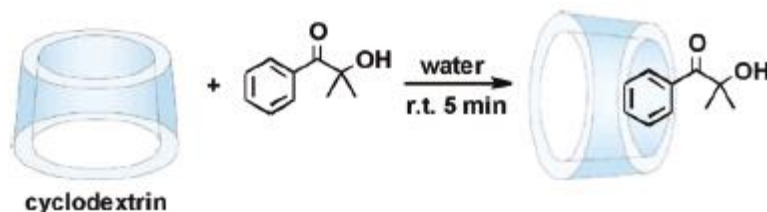
Figure 2.1 Water insoluble PI Becomes water soluble. Complexing with β-Cyclodextrin.

Source: Jeromin, Julia and Ritter, Helmut, "Cyclodextrins in Polymer Synthesis: Free Radical Polymerization of a N-Methacryloyl-11-aminoundecanoic Acid/β-Cyclodextrin Pseudorotaxane in an Aqueous Medium" Macromolecules, 32, 16 (1999): pp 5236–5239.

Although the focus of this study is primarily on acrylates, for environmental and health and safety considerations, it is important to note that epoxides and vinyl ethers are alternative monomers as they do not possess as strong an odor or eye and skin irritation issues [1]. However, as this is a cationic photoinitiated method of polymerization, it is important to discuss cationic PIs. The use of cationic PIs generally belong to three main classes: diazonium salts, onium salts and organometallic complexes [8]. The limitations associated with these compounds can include high toxicity and high cost because of their central heavy metals. It has been reported that long-term exposure to the counter ion of onium compounds, especially SbF_6^- and AsF_6^-, led to increased incidences of various cancers. Therefore, one must compare and contrast the benefits and more undesirable characteristics of the monomer(s)/oligomer(s) and photoinitiating system (PIS) before deciding on a final formulation.

Miao and Wang [9] reviewed vegetable oils and their inherent triglycerides as an important feedstock for polyurethanes, polyesters, polyethers and polyolefins known as vegetable-oil-based-polymers (VOBPs). The triglycerides are precursors for the monomers and have the potential to substitute petroleum-based biopolymers. These bio-polymers are important as their triglyceride based monomer selection could be carefully selected or tuned for the final formulation, with the resulting polymer possessing the desired mechanical properties based on that monomer selection. These materials could also be very useful oligomers in the photopolymerization process.

The authors reviewed data highlighting the key benefits with each VOBP. Polyurethanes are very versatile and have suitable properties for medical applications due to good biocompatibility and mechanical properties such as high tensile strength. Polyester thermosets, derived from a bio-based feedstock, with highly functionalized dicarboxylic anhydride/epoxy groups have been reported to have increased Tg and crosslinking densities, with Young's Modulus and tensile strength values reported as high as 1395 MPa and 45.8 MPa, respectively. Polyesters derived from just epoxidized soybean oil had values of just 65 MPA and 10.2 MPa, repectively. Polyethers, derived from vegetable oils, have an important application as bio-based surfactants, decreasing the surface tension of water to ~30mNm^{-1} at concentrations as low 0.07 wt. %. It is believed that these bio-based surfactants could be beneficial as dispersants in photopolymerizable suspension formulations, ensuring deagglomeration and small particle sizes yield stable homogenous suspensions for UV curing. Polyolefins possessing high chemical stability, good mechanical properties and biocompatibility are well established and have been applied for surgical applications since the 1950s. Polypropylene (PP) – acrylic block copolymers have

been used as additives in UV curable coatings and inks exhibiting good compatability between the polymers and no PP surface treatment required.

Marie and Bourret [10] investigated bio-polymer additives as ways of preparing stabilized alumina suspensions for tape-casting. Traditionally, these suspensions contain binders and plasticizers which are polymers coming from the petrochemical sector and may present environmental and/or operator health risks. Their aim was to identify sustainable additives with an end goal of substituting all additives sourced from the petrochemical industry, but adapt the biomaterials into formulations with respect to the resulting rheological and mechanical properties. The biomaterial-based additives incorporated were pectin as a binder, glycerol as a plasticizer, and ammonium lignosulfonate as a dispersant. The outcome of substituting eco-friendly additives into ceramic tape formulations was promising from a rheological and mechanical properties standpoint. The suspensions presented shear thinning behavior which is typically required for such a process, and the resulting tapes exhibited flexibility and mechanical resistance without defects as evidenced by electron microscopy.

Lu et al [11] investigated thermosetting acrylate resins derived from soybean oil for sheet molding compound (SMC) applications. Again, the push was to find a renewable resource for the raw materials. Soybean oil has been identified as one attractive renewable resource due to its abundance, and is used in industrial processes (mold releases, surfactants) and triglyceride composition. Acrylated epoxidized soybean oil has been identified as a rigid polymer attractive for SMC applications due to the C=C groups that would undergo Free Radical Initiated Polymerization (FRP), and the hydroxyl groups added from the acrylic acid (used in acrylation process) that can be further modified with

cyclic anhydrides yielding greater unsaturation. The synthesis routes to form Acrylated

Epoxidized Soyabean Oil (AESO) and oligomer triglycerides are depicted in Figure 2.2.
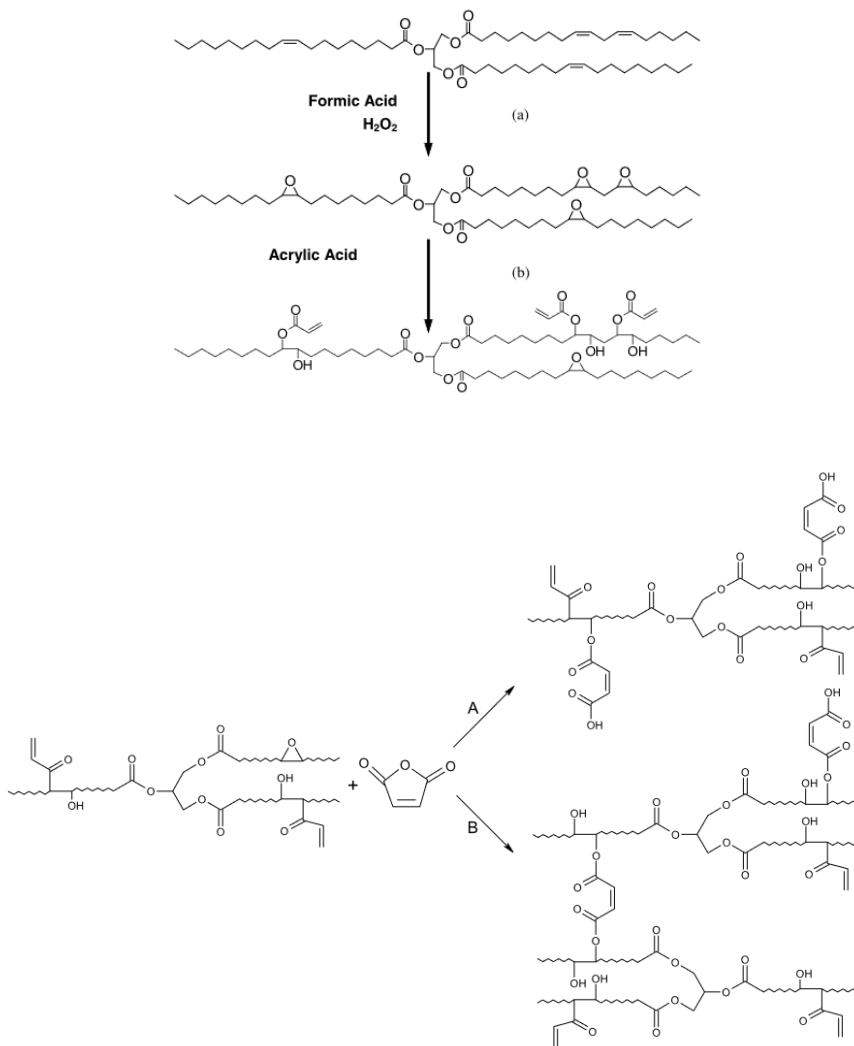
Figure 2.2 Acrylated epoxidized soybean oil triglyceride synthesis.

Source: Lu, Jue and Wool, Richard P. "New sheet molding compound resins from soybean oil. I. Synthesis and Characterization." 46, 1 (2005): 71-80.

The resulting monomers were copolymerized with 33 wt. % styrene to further

enhance rigidity within the polymers and meet the requirements for mechanical properties.

Dynamic mechanical analysis on these resulting polymers indicated modification with

maleic anhydride that introduced more cross-link sites to the triglyceride, more acid

functionality (necessary to the SMC process) and copolymerizing with styrene increased both the polymers moduli and Tg to temperatures above 100°C. The optimized styrene and triglyceride-based monomer was formulated to 33.3 wt.% styrene and 66.7 wt. % biorenewable monomer and showed significant promise for SMC applications.

Liu et al. [12] reported on a novel green approach to improving the mechanical performance and renewable content of natural vegetable oil-based UV-curable materials through the introduction of cashew nutshell liquid (CNL) into the plant oil backbone. Their group reports on formulating acrylated epoxidized soybean oil (AESO) based UV coatings and a UV curable branched oligomer based on CNL and ESO known as a soy-based UV-curable branched oligomer (ACSO), both of which were synthesized by chemical modification with acrylic acid to form an acrylated vegetable oil. Structurally, CNL contains a rigid benzene ring and more fatty unsaturated content with a shorter fatty chain than the triglyceride; therefore, it was believed CNL would play a role in imparting good mechanical properties. Upon UV irradiation, the ACSO polymer formed with CNL was reported to have a higher Tg and biorenewable content, with improved mechanical properties and thermal stability over the AESO.

Overall, positive environmental factors are associated with photointiatiated systems (low to no solvent use and ease of cleanup), particularly in aqueous media[7]. Further monomer/oligomer synthesis and formulation additives from renewable resources such as soybean oil and cashew nutshells demonstrate that UV chemistry is a superior technological source when compared to many conventional chemistry formulations.

2.2 Operating Principle

Radical and cationic photopolymerization reactions are largely encountered in industrial applications within ceramics and radiation curing and imaging areas [1]. Free radical polymerization (FRP) or free radical photopolymerization is the most used reaction for SLA applications. Monomers/oligomers with reactive vinyl unsaturation such as acrylates and methacrylates, mono- or polyfunctional diluents along with the PI are major ingredients of UV-curable formulations. These formulations are highly sensitive to UV irradiation and subsequently possess fast cure speeds as the liquid to solid phase change is immediate (~2s or less) upon intense radiation [13].

With respect to the Photo Initiating System (PIS), this key factor in photopolymerization reactions is responsible for allowing the starting resin formulation to absorb the light and to create reactive species that are further able to initiate the polymerization [14]. A typical PIS for free radical photopolymerization could consist of (i) a photoinitiator (PI; e.g., suitable cleavable ketones), (ii) a photoinitiator (e.g., a ketone) and a co-initiator (coI; e.g., an amine, a thiol, a silane, etc.), (iii) a photosensitizer (PS) and a PI or (iv) more complex associations such as PS/PI/coI/RS (where RS is a molecule that improves the efficiency through additional side reaction). The radicals, generated after the PIS system is irradiated with a light source (e.g. Hg lamp, Xe lamp, Hg-Xe lamp, LED, lasers, laser diodes, etc.), are responsible for initiating the polymerization as described in Figure 2.3.

$$PIS + \mathbf{h\nu} \rightarrow\rightarrow\rightarrow R\bullet \rightarrow Polymer \qquad\qquad (2.1)$$

Most PIs for free radical polymerization absorb in the UV wavelength and lead to the generation, upon excitation from a light source, of a radical initiating species ($R\bullet$) as expressed in (2.1). There has also been research exploring colored molecules, such as dyes or PS, which could play an interesting role in the PIS to absorb light and transfer their excitation to a traditional PI as expressed in the FRP reactions in (2.2) and (2.3).

$$PI + \mathbf{h\nu} \ (UV\ light) \rightarrow PI^* \rightarrow R\bullet \qquad\qquad (2.2)$$

$$PS + \mathbf{h\nu} \ (visible\ light) \rightarrow PS^* \rightarrow PI^* \rightarrow R\bullet \qquad\qquad (2.3)$$

$$PS + \mathbf{h\nu} \ (visible\ light) \rightarrow PS^* \rightarrow PS\bullet - + PI\bullet + \rightarrow R'\bullet \qquad\qquad (2.4)$$
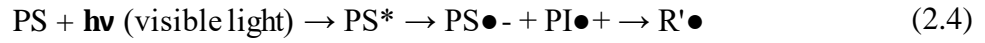
Photoinitiated polymerization is usually applied to a chain growth and/or crosslinking process where both the initiating species and the growing chain ends are radicals or ions (Figure 2.3). As can be seen by observation of Figure 2.3, light is responsible for the very first step in photopolymerization, namely absorption and generation of the initiating species. The photointiator (PI) plays a role in the polymerization reaction as it activates the monomer/oligomer to propagate and generate larger radicals, hence facilitating the chain growth. Pairing the light source and photoinitiator is important because curing lamps must emit UV energy in the spectral area that activates the PIs used in a formulation.
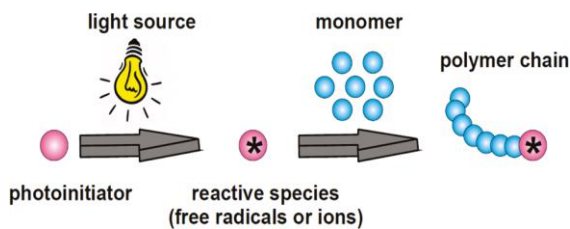
Figure 2.3. General presentation of photoinitiated polymerization.

PIs for UV curing are classified as type I (unimolecular cleavage) and type II (bimolecular abstraction or electron transfer). For this study, type I PIs for acrylate chemistry were the focus, namely acyl phosphine oxides and α-hydroxyalkyl ketones which spontaneously undergo "α-cleavage" generating free radicals after being irradiated with light from a UV lamp as depicted in Figure 2.4. Each PI has advantages and disadvantages, and the selection of PI depends on the requirements of a particular application. PIs affect mainly cure speed and cost, but other factors such as commercial availability, solubility in monomers, storage stability and cost should also be taken into consideration. The photointiators utilized in this study were supplied directly from a vendor and are known under chemical names as (BAPO- Bis(2,4,6-trimethyl benzoyl)phenyl phosphine oxide – solid, yellow powder) and Omnirad 2022 (a liquid blend of BAPO and α-hydroxyalkylketone). They were incorporated at about 7% wt./wt. of the formulation (2% wt./wt. BAPO and 5% wt./wt. α-hydroxyalkyl ketone, respectively).
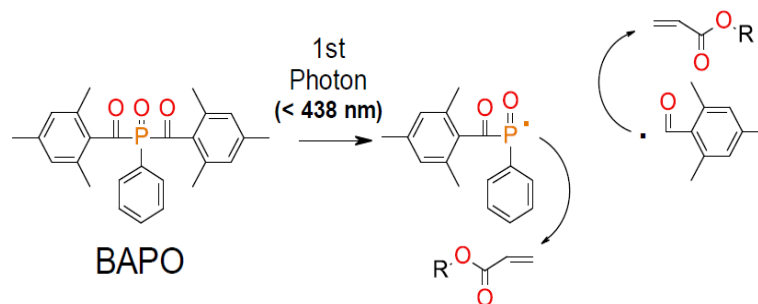
Figure 2.4. Bisacylphosphine oxide absorbing light to initiate polymerization.

Overall radical photopolymerization process of acrylates will occur in three stages: initiation, propagation and termination[10]. Initiation has been covered extensively within this section and is characterized more succinctly by the reaction (2.5) where PI* is the PIS that has undergone excitation after irradiation from a light source and generates two free radicals (as exemplified by BAPO in Figure 2.4).

$$PI + h\nu \rightarrow PI^* \rightarrow R_1\bullet + R_2\bullet \qquad (2.5)$$

One or both of the radicals ($R_1\bullet + R_2\bullet$) will combine with the monomer/oligomer (M) in the formulation, and subsequently generate a new radical RM which will propagate polymerization as described by (2.6).

$$R\bullet + M \rightarrow RM\bullet \qquad (2.6)$$

Propagation is the stage where successive addition of monomer/oligomer units on the growing chain takes place to generate larger radicals.

$$RM_n\bullet + M \rightarrow RM_{n+1}\bullet \qquad (2.7)$$

Finally, termination corresponds to the end of the photopolymerization process either via combination or disproportionation.

$$RM_{n+1}\bullet + RM_{n+1}\bullet \rightarrow \text{terminated polymer} \qquad (2.8)$$

Several analytical tools are utilized to characterize the conversion and rate of polymerization with a particular emphasis on Real-Time Infrared Spectroscopy (RTIR), Fourier Transform Infrared Spectroscopy (FTIR) and Raman Spectroscopy.

FRP is susceptible to molecular oxygen, a common inhibitor that will significantly hinder the rate of propagation. Inhibitors are molecules that can retard or prevent the polymerization reaction so that the radicals generated are unable to react with another monomer. Such molecules may be introduced to monomers that are being stored for periods of time, then removed by distillation or packed column when ready to use for polymerization reactions [16]. In another approach, inhibitors of polymerization have been used in continuous liquid interphase printing [2]. Inventors looking to provide a method of forming a 3D printable object with sufficient resolution and relative ease have developed commercial-off-the-shelf (COTS) 3D printers that utilize this concept when fabricating their printers. The printers include a zone which comprises a carrier, build surface and an

14

optically transparent resin tank (which holds the unpolymerized monomer) as seen in Figure 2.5. Within this zone, a build region exists which is defined as the area filled with unpolymerized monomer that is subsequently irradiated from below the optically transparent resin tank. However, not only light permeates through this optically transparent tank, it is also permeable to inhibitors of polymerization (e.g. oxygen) which are essential in the fabrication of three dimensional objects.
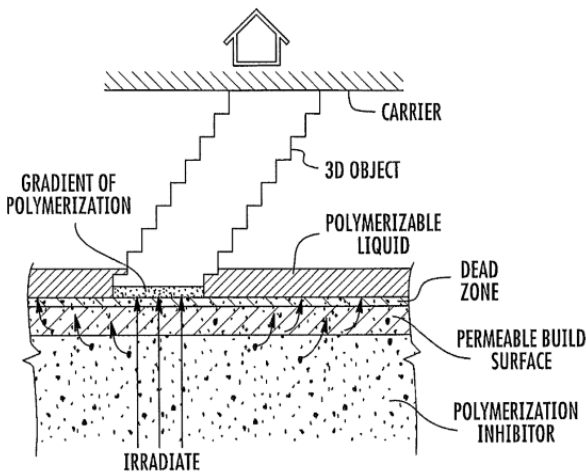
Figure 2.5 Diagram of an SLA 3D printer. This printer utilizes a bottom-up approach as the laser permeates the optically transparent build surface and initiates polymerization within the resin tank. The build surface is also permeable to oxygen which is claimed to allow polymerization inhibitor migrate through the resin tank.

Source: DeSimone, Joseph M.; Ermoshkin, Alexander; Ermoshkin, Nikita, Samulski, Edward T. "Continuous Liquid Interphase Printing." Redwood City, CA (US), 2016.

Essential to printing a final resin suspension, the formulation must be developed with a particular emphasis on homogeneity. The attritor mill is a simple and effective agitating ball-mill useful for decreasing particle size and deagglomeration within a suspension for batch or continuous operation. This mill has been widely used for preparing homogenous UV curable suspensions in the ceramic industry, and was utilized in this work

for similar purposes. The mill employs an overhead shaft with cross arms that rotate at high speed exposing the grinding media (stainless steel, chrome steel, tungsten carbide, ceramic or zirconium oxide) and rotating shaft to the material to be ground. The material of interest and the grinding media are placed in a stationary, jacketed grinding tank. The agitated media exert shearing and impact forces on the material, resulting in size reduction/agglomeration. Particle distribution can be easily controlled, and ingredients can be added directly to the grinding tank without premixing. A diagram of an attritor mill is displayed in Figure 2.6.
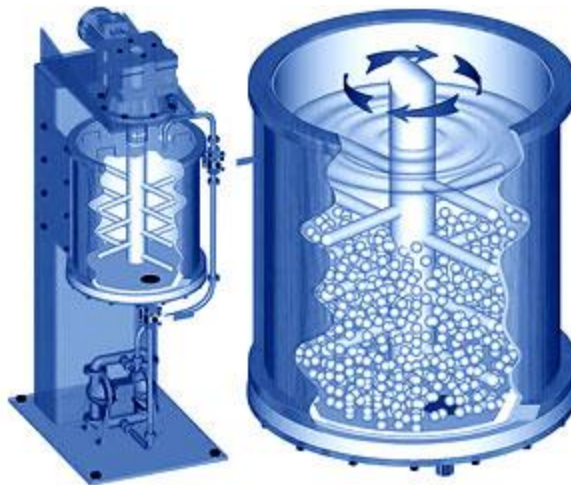
Figure 2.6 Diagram of an attritor mill.

Source: Mikrons Grinding & Dispersion Made Easy. How an Attritor Works?
http://attritor.in/attritor_working.html, accessed October 9th, 2009.

2.3 Mechanical Analyses

Dynamic Mechanical Analysis (DMA) utilizes an applied oscillating force to a sample and then subsequently measures the materials' response to that force [17]. The applied force, or stress (σ) a material is subjected to gives rise to deformation, or strain (ε). Simply by measuring stress and strain and plotting them on a Cartesian, one can calculate the modulus (stiffness), resistance to flow (viscosity), and the ability to recover from deformation

(elasticity). This is the basis for tensile testing. The stress-strain curves vary depending on many factors, and a simple analysis of a typical stress-strain curve is given in Figure 2.7. Since we are dealing with polymers, it is important to give an overview and depict several trends polymers display as a function of stress/strain. Figure 2.8 shows the effects of structural changes on stress-strain curves. For polymers, stress-strain curves change as temperature increases and as fillers are added to the polymer. As a polymer is heated, it becomes less brittle and more ductile. The same is true for the addition of plasticizers. However, when adding fillers, particularly powders, elongation and ultimate strength will decrease as the concentration of filler increases. There is also a maximum limit to the amount of filler that can be added to the polymer while still maintaining the desired mechanical properties. If there is not enough polymer matrix to hold the composite together, the material is useless.
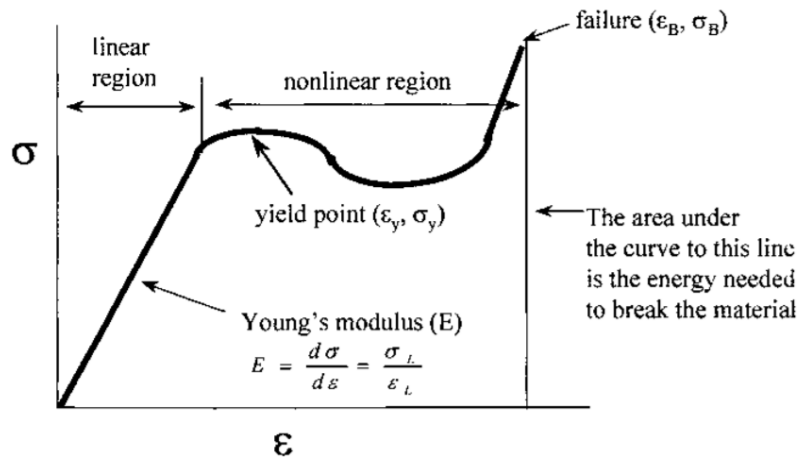
Figure 2.7 Typical stress-strain curve as shown by extension.

Source: Menard, Kevin P. Dynamic Mechanical Analysis: A Practical Introduction. Boca Raton: CRC Press, 1999.

A material under sinusoidal stress, as in a dynamic analysis, exhibits a certain amount of strain corresponding to the elastic response (as long as the material is kept in its linear viscoelastic region). If the material deforms with the applied stress as a perfectly

elastic solid, then there is an in-phase response. A purely viscous material would give an out-of-phase response as molecular motion, entanglements, etc. within the polymer sample and would give rise to a phase lag between the applied stress and measured strain. A viscoelastic material lies somewhere in between. This is exemplified in Figure 2.9. The difference in phase angle δ corresponds to the difference between the applied stress and resultant strain. This allows a modulus data point to be broken into two terms, one related to the storage of energy (E') which quantifies the elasticity of the polymer, sometimes referred to as the in-phase or storage modulus, and another term (E") which quantifies the viscous behavior or the energy loss in internal motion arising from viscous behavior. E' and E" can be calculated as follows from Equation (2.1) and (2.2).
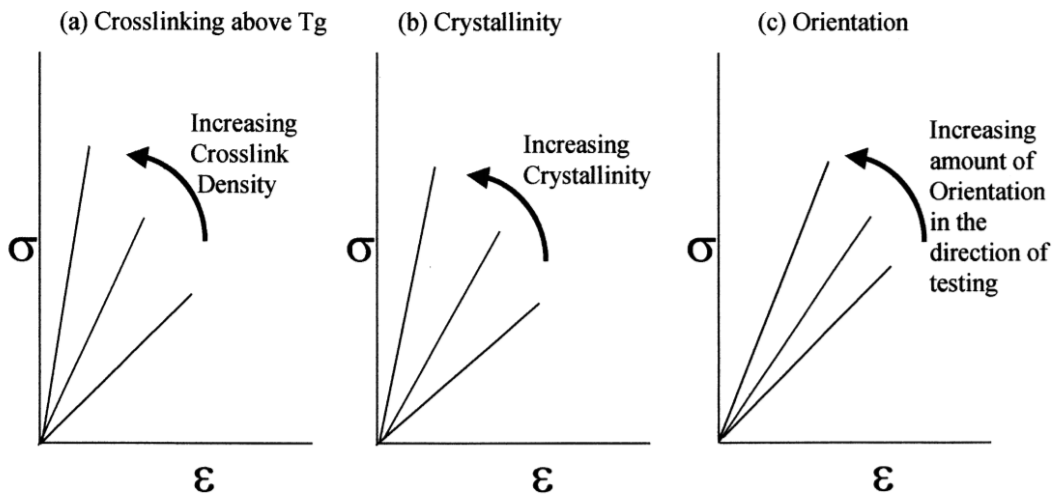
Figure 2.8 Effects of polymer structural changes on stress-strain curves.

Source: Menard, Kevin P. Dynamic Mechanical Analysis: A Practical Introduction. Boca Raton: CRC Press, 1999.

$$E' = \left(\sigma^{\circ}/\varepsilon^{\circ}\right)\cos\delta = \left(f_{o}/b\mathbf{k}\right)\cos\delta \qquad 2.1$$

$$E'' = \left(\sigma^{\circ}/\varepsilon^{\circ}\right)\sin\delta = \left(f_{o}/b\mathbf{k}\right)\sin\delta \qquad 2.2$$

where δ is the phase angle, b is the sample geometry term, f_0 is the force applied at the peak of the sine wave, and k is the sample displacement at the peak.
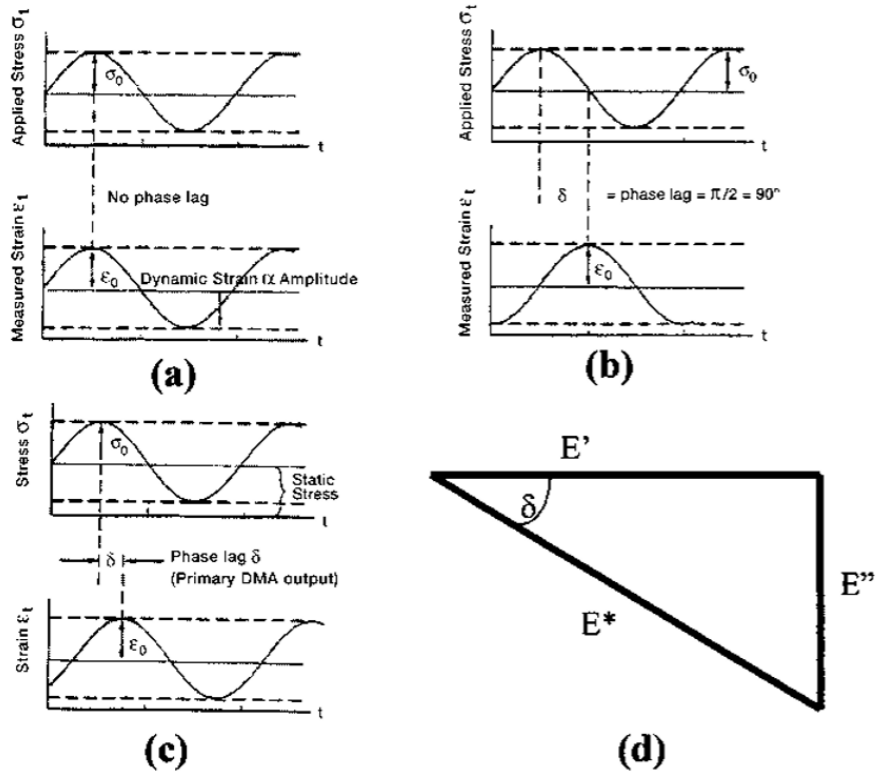
Figure 2.9 Material response to applied stress. Elastic solids give an in-phase response as is seen in (a). Purely viscous materials give an out of phase response (b), and viscoelastic materials fall in between (c). The relationship between phase angle and E is given in (d).

Source: Menard, Kevin P. Dynamic Mechanical Analysis: A Practical Introduction. Boca Raton: CRC Press, 1999.

The thermal transitions in polymers that are subjected to DMA have been described in terms of free volume. Changes in free volume are connected to loss of stiffness, increased flow and change in relaxation time; and these changes arise from intrinsic polymer properties such as viscoelasticity, aging and impact properties. From this description, the various transitions that polymers undergo can be characterized and this process is exemplified in Figure 2.10. With increase in temperature, the molecules

transition from being tightly compressed with limited free volume, to more mobile segments having the ability to move in various directions characterized by bending and stretching. Continued heating and a further increase in free volume enables the glass transition temperature (T_g) of the amorphous polymer to be reached, which is characterized by large scale motions of polymer chains. This stage has been described by many as a major transition where the polymer material goes from being hard and glassy to a rubbery state. As heating continues, the sample passes through the rubbery plateau, associated with chain entanglements and crosslinks between polymer segments. Finally, thermoplastic samples will transition through the melting temperature (T_m); which is characterized by chain slippage and material flow. This behavior is a function of molecular weight. Importantly, thermosets experience no T_m as crosslinks and molecular weight prevent chain slippage. When high enough temperatures are met, burn and degradation occurs.
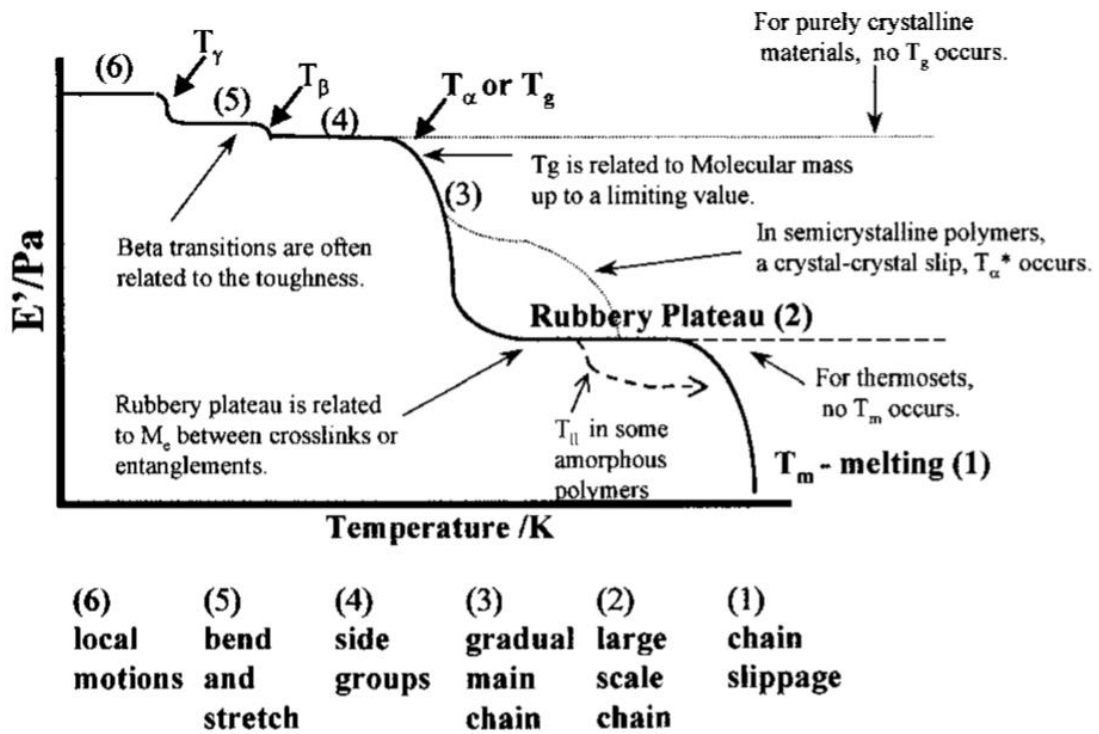
Figure 2.10 Ideal DMA temperature ramp of a polymer. Starting with low temperatures on the left. The scan moves from very low temperatures and passes through solid state transitions as the temperature increases; the warming is associated with free volume increase and localized polymer bond rotations/bends/stretching.

Source: Menard, Kevin P. Dynamic Mechanical Analysis: A Practical Introduction. Boca Raton: CRC Press, 1999.

CHAPTER 3
LITERATURE OVREVIEW AND PRESENT STATUS

In this section, photoinitiated polymerization and SLA results from the literature will be explored with an emphasis on studies involving solids from the ceramics industry. The focus will be on suspensions of acrylate monomers and experimental techniques for reducing/deagglomerating particles and some of the analytical techniques that are deployed for the determination of cure kinetics, mechanical properties and rheological determinations.

For more than 30 years, photointitated polymerization has been the basis for conventional industrial applications in coatings, adhesives, inks, printing plates, optical waveguides, and microelectronics [1]. Other studies, involving various photopolymerization processes, have been conducted in biomaterials for bones and tissue engineering, microchips, curing of acrylate dental fillings, optical resins and recording media, clay and metal nanocomposites, photoresponsive polymers, liquid crystalline materials, interpenetrated networks, microlenses, multilayers, surface modification, block and graft copolymerization, living/controlled polymerization, interfacial polymerization, and so forth. In contrast to thermally-cured polymers (often requiring elevated temperatures), photopolymerization can be performed at room temperature or lower. Additionally, these monomers are often readily polymerizable and used for applications in which heating is unacceptable such as dental fillings or energetic materials.

3.1 Additive Manufacturing and SLA Printing

Chartier et al. [13] evaluated the respective contribution to the rheology of suspensions containing different concentrations of SiO_2 ($d_{50} = 2.25\mu m$) and the influence of the rheology of the intergranular reactive phase on the photopolymerization (measurement of the kinetics of conversion and the conversion rate). They also evaluated the influence of changing powder concentrations on UV reactivity with respect to parameters such as polymerized thickness (E_p) and polymerized width (L_p). The UV curable system consisted of a PI (2,2-dimethoxy-1,2-phenylacetophenone (DMPA)) with a reactive amine modified polyester acrylate (PEAAM) and 1,6 hexanediol diacrylate (HDDA) as a diluent monomer. The suspensions were prepared by attrition utilizing 1 mm diameter zirconia media and varying wt. % of a phosphate ester dispersant. The rheological changes, induced by particle-monomer and particle-particle interactions at concentrations above 10 vol. %, decrease the % conversion of the suspensions as well as the polymerization rate. This was believed to be due to the increase in viscosity associated with the evolution of polymer chains which subsequently generates a "resistance" to the diffusion of the radical species formed during propagation which are essential in polymer formation. At higher concentrations of solids loading (>10 vol. %), the challenge remains to be able to maintain the viscosity of the continuous phase low enough so that it is flowable while preserving the photoreactivity of the suspension.

E_p and L_p were determined by spreading the uncured silica suspensions with varying concentrations (5-50 vol. %) onto a fabrication plate with known dimensions, curing with a 353nm wavelength argon ionized laser with 1W maximum output power and cutting the resulting polymer into filaments. By utilizing an optical microscope with a camera and the necessary software, E_p and L_p could be measured. As expected, E_p

decreased with increasing concentration of silica due to smaller penetration of the laser beam (D_P) caused by particle light scattering. On the other hand, L_P which represents dimensional resolution (one of the key attributes to SLA techniques in AM) is increasing. This challenge is directly associated with the addition of solid particles to monomers; the reactivity to UV of the suspension is critical for polymer formation and was found to be in agreement with the Beer-Lambert law. As silica concentration is increased, less light energy is absorbed by the system to generate radicals; therefore, the energy necessary for the polymerization is decreasing which is evident by decreased polymer thickness at higher silica concentrations.

Griffith and Halloran [18] investigated SLA methods involving the incorporation of differing volumes of ceramic materials (silica (SiO_2) and alumina (Al_2O_3)) into a curable solution with a focus on cure thickness and viscosity control to produce a high quality ceramic formulation. Preliminary work revealed that cure depth was controlled by particle size and the difference in refractive index between the ceramic and the ultraviolet solution. The systems investigated were fluid suspensions with both ceramic materials as the solid phase and 30 wt. % acrylamide and 70 wt.% crosslinking monomer methylene bis-acrylamide in the liquid phase. The PIS involved was 0.4w/o phosphine oxide with 0.7 w/o ketone derivative. The lamp incorporated was a medium pressure mercury UV lamp with a max irradiance density of 2.51 W/cm^2. UV curing of both ceramic suspensions at high volume percent solids revealed that depth of cure (D_c) was greater when the ceramic particle sizes were smaller indicating that DC is inversely proportional to the particle size. A standard expression for the turbidity of suspensions was postulated to be a predictor for the cure depth for any ceramic powder in any UV curable suspension based on the differences between refractive indices of monomers and ceramic particles under UV light.

This was based on the observation at higher vol. %; larger values for D_c were quantified for silica (refractive index RI = 1.56) than alumina (RI = 1.7). More testing with different monomers and ceramics was to be carried out to increase D_C.

Chartier and Dupas [19] investigated and evaluated the influence of processing parameters (laser power, scanning speed, number of irradiations, and the impact of irradiation of subsequent upper layers onto the previously deposited/irradiated layers) on the degree of polymerization by Fourier Transform Infrared Spectroscopy (FTIR) and Raman spectroscopy within an SLA printer. These spectroscopic methods are commonly utilized in the polymer industry to determine the final degree of polymerization due to characteristic acrylate double bond stretching being proportional to bond concentration; hence one can follow the evolution of polymerization as the double bond is the reactive site on the monomers, but is non-existent once the polymer is formed. The monomers chosen were Hexanediol Diacrylate (HDDA) and pentaerythritol tetracrylate (PPTTA) in a 10% PPTTA/90% HDDA ratio and Dimethoxy phenylacetophenone (DMPA) as a PI. The ceramic was alumina with a mean particle size of 0.5µm. The formulation was ball milled with the aid of a dispersant and thin layers with a fixed 50 µm thickness were prepared for multilayer (2 -12 layers) sample preparation. The results obtained indicated that layer thickness had a direct effect on the degree of conversion between the sides of each layer, and up to several layers can be affected by the irradiation of the subsequent upper layers. This phenomenon was associated with inhomogeneous polymerization meaning internal stresses become favorable and the risk of crack propagation and/or deformation could be inevitable. Constant and reduced energy density irradiation with a low scanning speed were favorable processing parameters for reaching homogeneous polymerization.

Badev and Abouliatim et al [20] investigated the photoinitiated polymerization of a commercial amine modified polyether acrylate oligomer with HDDA as the diluent and DMPA as the PI. RTIR was utilized to study the effect of light intensity, PI concentration, and diluent concentration in the homogenous phase. Next, ceramic fillers (SiO_2, Al_2O_3 (three different P.S.), ZrO_2 and SiC) were attritor-milled and added to form suspensions; then the resulting kinetics of polymer conversion was characterized. The nature of the discontinuous ceramic phase, the particle size and concentration, as well as subsequent viscosity increase, upon formation of the suspension, were the main parameters controlling reaction rates. HDDA as a diluent (concentrations 10-15 vol. %) was found to enhance double bond conversion as evidenced by RTIR confirming viscosity control as one of the main parameters governing the polymerization reaction. Light propagation behavior, in agreement with Griffith and Halloran [18], showed that the difference in refractive index between acrylate monomers and ceramic particles was responsible for the decrease in converted final polymer (and polymerization rate) as solids loading is increased. With respect to particle size, decreased particle size induced a deterioration in final conversion to polymer, attributed mostly to light scattering affects.

Lei and Frazier [21] utilized DMA in tensile-torsion mode to predict the curing behavior of a phenol-formaldehyde (PF) composite resin on paper adhesive emphasizing stability during the cure. The strain curves were used to identify the onset of curing temperature and cure degree (thermally activated cure, not photoinitiated), and the cure behavior of the resin was calculated by combining the G', tan δ, and strain curves. The DMA was operated in torsion mode with a fixed frequency at 0.5 Hz. The prepared samples were initially pre-cured at 60°C for 60 min. and subjected to temperature ramps

(25-180°C; 5°C, 10°C and 15°C/min and oscillation stress = 10MPa) with at least three
replications being conducted.

Figure 3.1 DMA Temperature ramp of PF composite.

Source: Lei, Hong; and Frazier, Charles E. "A dynamic mechanical analysis method for predicting curing behavior of phenol-formaldehyde resin adhesive," Journal of Adhesion Science and Technology, 29, 10 (2015): 981-990.

By analyzing the temperature ramp of the paper impregnated with PF resin (Figure 3.1), the significant reduction in G' values observed were indicative of substantial softening of the polymer up to about 60°C. This was where the storage modulus leveled off at a minimum plateau due to crosslinking effects. The G' value stayed fairly constant until the temperature reached about 125°C and the gelation point (T_{gel}) was reached, characterized by an abrupt increase in G' or the maxima of the tan δ curve.

From the strain curve, it was evident to researchers that strain was increasing complement to resin softening until 108.9°C, at which the strain reached a maximum. This temperature was indicative of mechanical cure within the polymer chains overtaking the physical effects of resin softening and was taken to be an accurate measurement of curing temperature (T_{cur}) due to its simplicity and clarity.
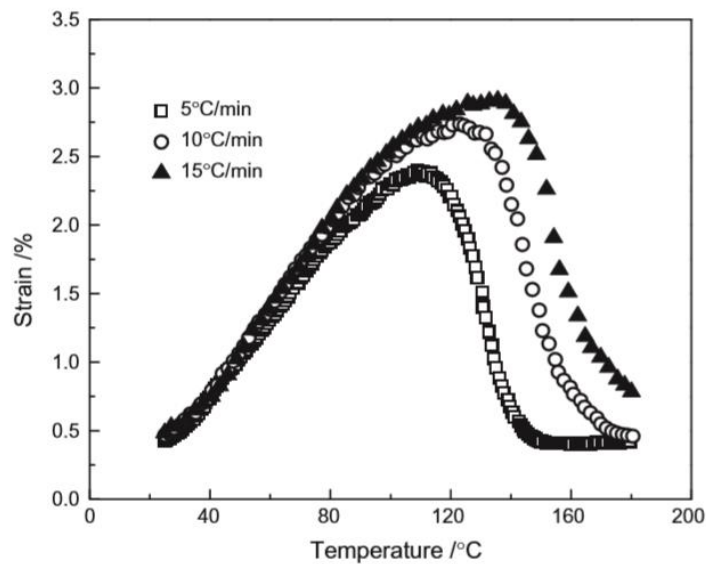
Figure 3.2 PF composites subjected to differing heating rates. The shift to the right is in agreement with the time-temperature superposition theory.
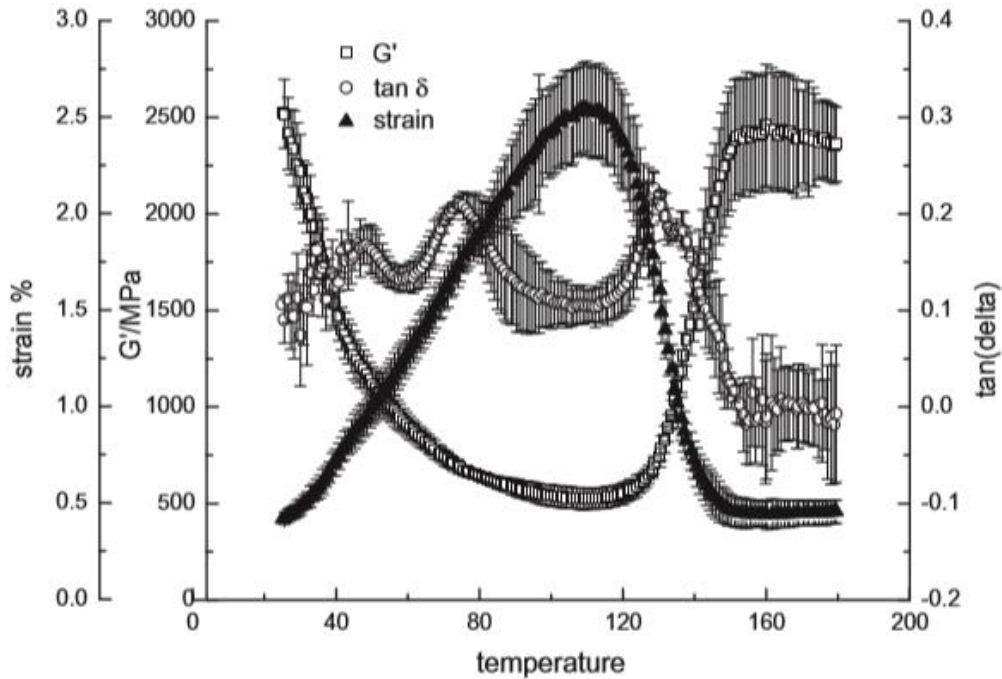
Source: Lei, Hong; and Frazier, Charles E. "A dynamic mechanical analysis method for predicting curing behavior of phenol-formaldehyde resin adhesive," Journal of Adhesion Science and Technology, 29 (10) 2015: 981-990.

In Figure 3.2, the strain curves of the PF composite specimens were subjected to different heating rates. Subsequently, the increase in heating rate from 5 to 15°C/min. shifted the T_{cur} as explained by the time-temperature superposition theory (see APPENDIX A) where the increased heating rate could be viewed as an increase in test frequency or a shortening of the observation time. By utilizing G' or strain curves from DMA, the authors were able to calculate the curing degree, β of a resin at time t by the following:

$$\beta = \frac{G'(t) - G'_{\text{min}}}{G'_{\text{max}} - G'_{\text{min}}} \tag{3.1}$$

where G'_{min}, G'_{max} and $G'(t)$ are the minimum G', maximum G', and G' at time t during the curing process, respectively. Curing degree could also be calculated by strain curves (seen as a more accurate method for determining the onset point) as seen below:

$$\beta = \frac{A(T) - A(T_{\text{cur}})}{A - A(T_{\text{cur}})} \tag{3.2}$$

where, A(T) was the integral area from the beginning of testing (25C°) to a temperature, T on the temperature/strain curve where T was higher than T_{cur}, A(T_{cur}) was the integral area from the beginning temperature to T_{cur}, and A was the total integral during the entire temperature scan. The average degree of curing of the resin could then be calculated based on Equation 3.2, and was plotted in Figure 3.3 for two different heating rates (5 and 10 °C/min). It was clear to researchers that, with a lower heating rate, the resin would get completely cured at a lower temperature.
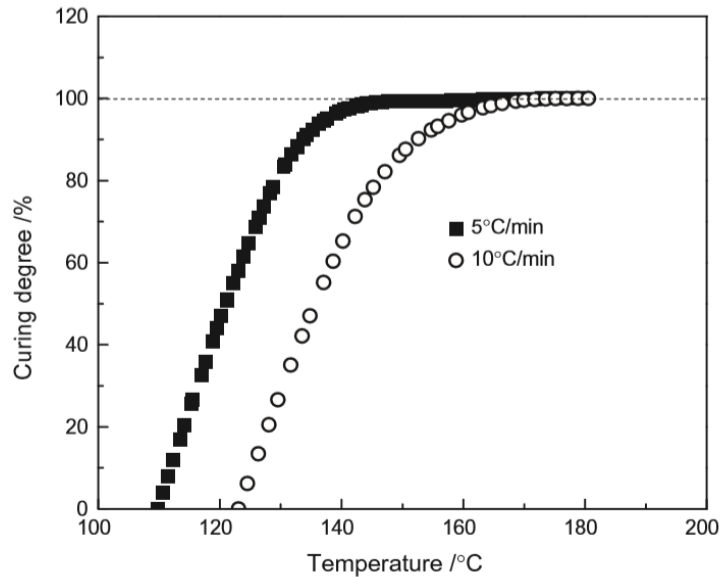
Figure 3.3 Curing degree as a function of heating rate. A full degree of cure could be reached with a slower heating rate at a lower temperature.

Source: Lei, Hong; and Frazier, Charles E. "A dynamic mechanical analysis method for predicting curing behavior of phenol-formaldehyde resin adhesive," Journal of Adhesion Science and Technology, 29 (10) 2015: 981-990.

Overall, the researchers showed that DMA in tensile-torsion mode was a suitable method for monitoring cure behavior and onset of curing temperature through G' and strain curves. The integral area under strain curves was demonstrated to be a good method for calculating curing degree. It was further shown that the combination of G', tan δ and strain curves was a valuable and comprehensive method for investigating cure behavior.
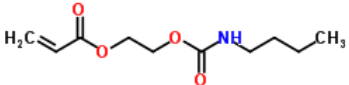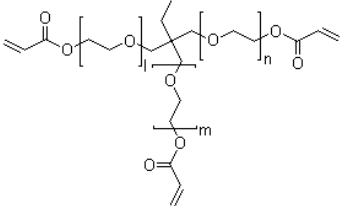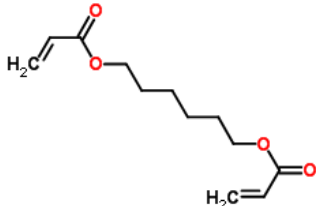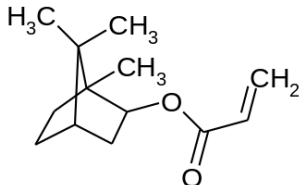
CHAPTER 4

PREPARATION AND CHARACTERIZATION OF THE UV-CURABLE FORMULATIONS

4.1 Formulation Preparation

A list of monomers chosen for this study are summarized in Table 4.1.

Table 4.1 Monomers/Oligomers from IGM Resins Used for Formulation Development

Chemical Name	Structure	Additional
2-[[(butylamino)carbonyl]oxy]ethyl acrylate		Monofunctional urethane acrylate, diluent, monomer
Ethoxylated (3) trimethylolpropane triacrylate		Aliphatic trifunctional acrylate
Aliphatic urethane tri-Acrylate	Proprietary	High viscosity, oligomer
Glycerol propylene glycol ether (1:3), mixed acrylates and adipates	Mixture	Tetra functional polyester acrylate oligomer, low viscosity
Acrylated aliphatic urethane	Proprietary	Aliphatic urethane, low viscosity. Oligomer
1,6-Hexanediol Diacrylate		Low viscosity diluent, di-functional monomer
Isobornyl Acrylate (IBOA)		Monofunctional monomer, high flexibility, low viscosity diluent

The monomers and oligomers utilized in the different formulations were supplied by IGM Resins, and had varying structures, functionalities, molecular weights, glass transition temperature (Tg), hardness, adhesion properties, and wetting capabilities. The properties of the resins were important in considering that a suspension was to be formed having an inert solid (melamine) of various particle sizes and solids loadings suspended within. Furthermore, the solids should ideally be homogenously dispersed throughout the resin, requiring the addition of dispersing agents and viscosity modifiers in some instances. Another aspect of the suspension formulation was the solubility of the suspended particle with the resin as this could lead to potential aggregation and larger solid particles via Ostwald ripening, and other instabilities that could interfere with the polymerization.

The objective of this study was to evaluate the formulation ingredients (inert acrylate monomers and oligomers) and form suspensions with inert solids (melamine) to propose ingredients for a candidate formulation that ultimately meets stability criteria and would have the potential to translate to energetic materials. The desired parameters on stability focused on particle size of the suspended solid, rheology, addition of stabilizers, diluents, dispersants/wetting agents/coupling agents, photoinitiators, monomer and oligomer chemical structures, solids loading within the resins and the conditions that can affect mechanical properties and ultimately, innovate propulsion charge design to meet new demands for increased performance.

4.2 Formulation Preparation for Mechanical Testing

Eleven mixes, having varying amounts of melamine loaded into several formulations of UV curable resins, were prepared. The mixtures prepared are outlined in Table 4.3. To add the melamine to the resins, a SpeedMixer (FlackTek) was used. The appropriate ratios of resin and melamine were added to the disposable containers of the lab size batch mixer,

and mixed at 3000 rpm for 3 minutes under vacuum. All the formulations were well-mixed, and the melamine was fully wetted into the resins without agglomeration, air bubbles or inhomogeneity. After mixing, these samples were transferred into a mold of rectangular shaped geometry and cured with a FireEdge FE200 Solid State UV LED Curing lamp manufactured by Phoseon. The Peak Irradiance was 2.0 W/cm^2, and the dominant wavelength was 395 nm.

The melamine was supplied by Sigma Aldrich and the particle size was measured using a Cilas 1190 laser particle sizer operating in liquid dispersion mode incorporating sonication. The particle size analysis (PSA) is shown in Figure 4.1, and the results are summarized in Table 4.2.
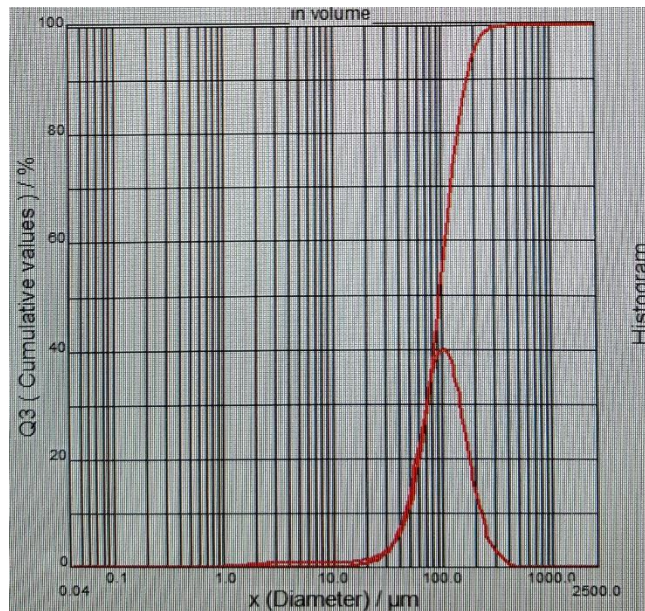
Figure 4.1 PSA of melamine measured in water with sonication.

Table 4.2 Distribution of Particle Size of Melamine.

Diameter at 10%	Diameter at 50%	Diameter at 90%	Mean Diameter
47.47 µm	95.19 µm	174.19µm	104.39 µm

Table 4.3 Formulations Investigated by DMA

Run	Name	Resin	Solids (melamine)	Comments
		wt/wt %	wt/wt %	
Mix 1	FLGPCL02	50%	50%	melamine d(0.9) 174.09μm (assuming no agglomeration)
Mix 2	FLGPCL02	25%	75%	melamine d(0.9) 174.09μm (assuming no agglomeration)
Mix 3	DB-1	50%	50%	melamine d(0.9) 174.09μm (assuming no agglomeration)
Mix 4	DB-1	25%	75%	melamine d(0.9) 174.09μm (assuming no agglomeration)
Mix 5	DB-6	65%	35%	milled melamine ~10 μm
Mix 6	JR-1	100%	0%	no solids
Mix 7	JR-1	50%	50%	melamine d(0.9) 174.09μm (assuming no agglomeration)
Mix 8	JR-1	25%	75%	melamine d(0.9) 174.09μm (assuming no agglomeration)
Mix 9	JR-2	100%	0%	no solids
Mix 10	JR-3	100%	0%	no solids
Mix 11	FLGPCL02	100%	0%	no solids

FLGPCL02 was a fully formulated resin purchased from Formlabs known as Clear Photoreactive resin. This resin was chosen as FormLabs recommended it for superior mechanical properties. From the safety data sheet (SDS), we knew that this was a blend of proprietary methacrylated monomers, oligomers and PIs. The JR-1 through JR-3 formulations were 50% IBoA and 50% proprietary aliphatic urethane triacrylate oligomer. For DB-1, there was about 30% of the same aliphatic urethane triacrylate oligomer, 10%

of the monofunctional urethane acrylate monomer, 33% of the aliphatic trifunctional acrylate, and 20% of a di-functional diluent, 1,6 hexanediol diacrylate, which was added to keep the viscosity of the resin lower and promote flow when added to the SLA tank. This formulation approach was recommended by the vendor. The oligomer was extremely viscous at room temperature and had to be heated to 60°C to reduce viscosity to about 3,000 mPa·s, which is close to the maximum viscosity for an SLA tank. As the blend of monomers and oligomer cooled for DB-1, the viscosity started to increase. Therefore, 20 wt. % of 1,6 hexanediol diacrylate was added to reduce viscosity.

DB-6 incorporated melamine that was milled in an agitated style batch ball mill consistent with the design of an attritor mill. The addition of a polymeric dispersant, supplied by Lubrizol, was added and recommended to be beneficial for organic material particle size reduction in UV cured formulations. First, the monomers/oligomers were blended together with the aid of an overheard stirrer, and the addition of the PI and dispersant were performed while the mixture was warmed to about 50°C. After cooling, the melamine was added and hand-mixed to ensure that it was wetted within the resin, then poured into the stationary, jacketed grinding tank with ceramic grinding media of the ball mill. The mixture was milled in the dark for about an hour, then imaged within an SEM (see Figure 4.1.2). The sample was prepared by dissolving a quantity of the resin suspension in isopropanol (IPA), then pipetting it onto a watch glass and allowing the IPA to evaporate within a fume hood. As the IPA and resin mixture evaporated, mostly the milled melamine sample was left on the watch glass due to the low solubility of melamine in IPA.
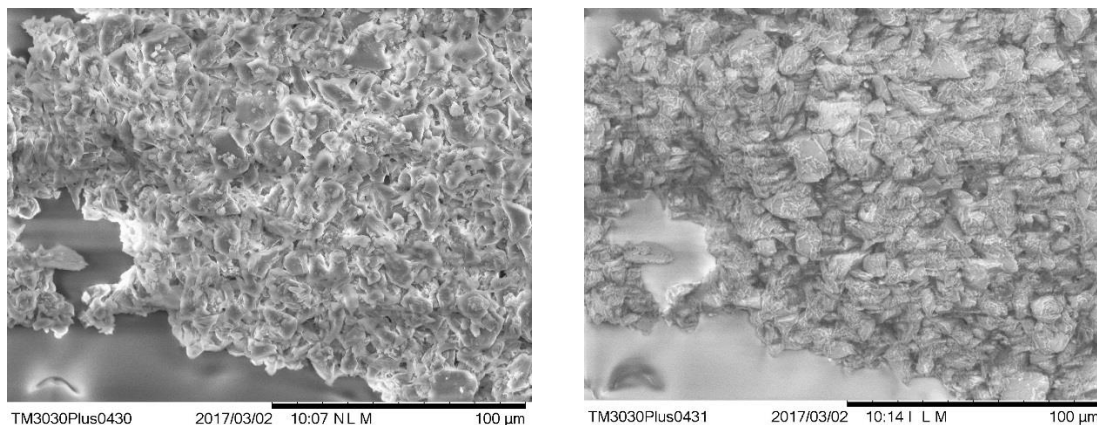
Figure 4.2 SEM image of milled melamine taken from resin suspension. The particle size is a d(0.9) of ~10μm.

Dynamic Mechanical Analysis (DMA) has been widely used to investigate and characterize the relaxation behaviors of polymeric materials since it provides information about changes in the state of atomic and molecular motion with varying temperature and frequency [17]. DMA (Q800 V21.3 Build 96) was run twice in multi-frequency strain mode to investigate the thermo-physical properties of the polymer formulations. The temperature was equilibrated at -150.00°C, then held isothermally for 5 min, and subsequently ramped at 2.00°C/min to 200°C at a frequency of 1 Hz. The formulations listed in Table 4.3 utilized DMA to further characterize the Tg of polymers (taken as peaks in the loss modulus (E")) and how the formulation compositions (monomers, oligomers, solids loading, different cross-linking, side chains, orientation) influence the formation of a polymer network structure. This is considered as critical information to the polymer formulator because, above the critical molecular weight (M^c), the mechanical properties dictate the performance of propellants; therefore, ingredient choice of formulation is crucial [17].

Tensile testing has been extensively used to explore a material's response to uniaxial loading. The test can provide information about a material's elastic modulus,

fracture point and yield strength; it has been widely utilized by industry for quality control purposes and predictions on behavior within specific applications due to stresses [22]. Tensile tests were performed using a benchtop Instron (Pneumatic grip control) testing machine, with a load cell maximum load of 100N. The formulations, listed in Table 4.4, utilized tensile testing to coincide with DMA and further characterize how formulation compositions and cure conditions affect the resulting polymer. The uniaxial tensile test experiments were performed at room temperature (25°C). The strain rate used was 5 mm sec^{-1}. The load (N), time (seconds) and elongation (mm) were recorded and subsequently converted to stress, ε and strain, σ, which were calculated using the cross-sectional areas and lengths of the specimens (Table 4.5)

For tensile testing, six samples were prepared in triplicate with varying solids loading into an optimized version of the DB UV curable resins. The mixtures prepared are outlined in Table 4.4. The continuous phase of the DB resin contained 50 wt.% IBoA, and 50 wt. % of the low viscosity tetrafunctional polyester acrylate oligomer. The suspensions were prepared by adding the melamine to the resin blend and homogenizing with an IKA ® ULTRA-TURRAX ® disperser tool. After mixing, the samples were transferred into dog-bone mold (see Figure 4.3) having rectangular geometry and cured with the same UV LED Curing Lamp utilized for the DMA samples.

Table 4.4 Formulations Prepared for Tensile Testing

Run	Name	Resin	Solids (melamine)	Comments
		wt/wt %	wt/wt %	
Mix 1	DB 7	50%	50%	melamine d(0.9) 174.09μm (assuming no agglomeration)
Mix 2	DB 7	60%	40%	melamine d(0.9) 174.09μm (assuming no agglomeration)
Mix 3	DB 7	70%	30%	melamine d(0.9) 174.09μm (assuming no agglomeration)
Mix 4	DB 7	80%	20%	melamine d(0.9) 174.09μm (assuming no agglomeration)
Mix 5	DB 7	90%	10%	melamine d(0.9) 174.09μm (assuming no agglomeration)
Mix 6	DB 7	100%	0%	no solids

Table 4.5 Dimensions of the Samples Prepared by Dog Bone Molds.

Sample	Length (mm)	Thickness (mm)	Width (mm)
DB (no solids)	25.1	0.78	13.2
DB(10wt.%solids)	38.1	2.05	12.9
DB (20 wt.% solids)	25.0	1.00	13.0
DB (20 wt.% solids)	25.0	1.30	13.8
DB (30 wt.% solids)	25.0	1.00	13.0
DB (30 wt.% solids)	96.5	1.65	12.3
DB (40 wt.% solids)	120.0	1.06	12.9
DB (50 wt.% solids)	76.2	1.00	13.2

Figure 4.3 Dog bone mold utilized for tensile testing of polymer samples.

CHAPTER 5

RESULTS AND DISCUSSION

The purpose of this chapter is to evaluate the formulations of interest and determine their ability to print in a COTS printer, and systematically evaluate the key ingredients in listed formulations. The key components of interest are the monomers/oligomers, the structure and functional groups they possess, their interaction with suspended melamine and the mechanical properties of the resulting polymer formed. Acrylate monomers cure very fast, and COTS 3D printers, utilizing LED lasers, present a good platform for 3D printing a complex geometry. Suspending solid particles into an acrylate resin can introduce a major challenge in terms of still printing a complex geometry. This is related to cure phenomena and particles scattering light resulting in an increase in L_P and decrease in E_P. Optimizing the monomer suspension is crucial for the design of a complex geometry polymer composite. With this optimization in mind, the first experiment involved introducing a foreign monomer/oligomer blend (not formulated by Formlabs) into the resin tank of a Formlabs 1+ 3D printer, and verifying that the formulation is 3D printable. The second set of experiments consisted of taking various formulations, and loading varied amounts of melamine into the formulation and testing the resulting mechanical properties after UV curing to form a polymer. The samples for mechanical analyses were prepared using molds and were cured with UV light. DMA testing enabled the formulator the ability to get vital information relating to cure behavior and how solid particles restrict polymer chain movement, resulting in Tg observance and Tg shifting resulting from post cure within multiple runs of DMA. Tensile testing has been extensively explored for quality control and can provide a benchmark for tuning the desired mechanical properties. Comparisons

between tensile data of new formulations and legacy materials could drive and innovate new synergetic formulations for optimization and enhanced performance.

5.1 Capability of Optimized Resin to Print in COTS 3D Printer

Approximately 300mL of DB-1 was poured into a Form 1+ SLA tank that utilizes a 405nm violet laser with an intensity of 120mW. The Formlabs printer utilized an upside-down (inverted) SLA process to print and it was successful in printing (though not recommended by Formlabs) when a foreign resin not formulated by them was introduced into the SLA tank. Some of the prints suffered from poor resolution and they stuck to the polycarbonate/silicone resin tank as seen in **Figure 5.1**.
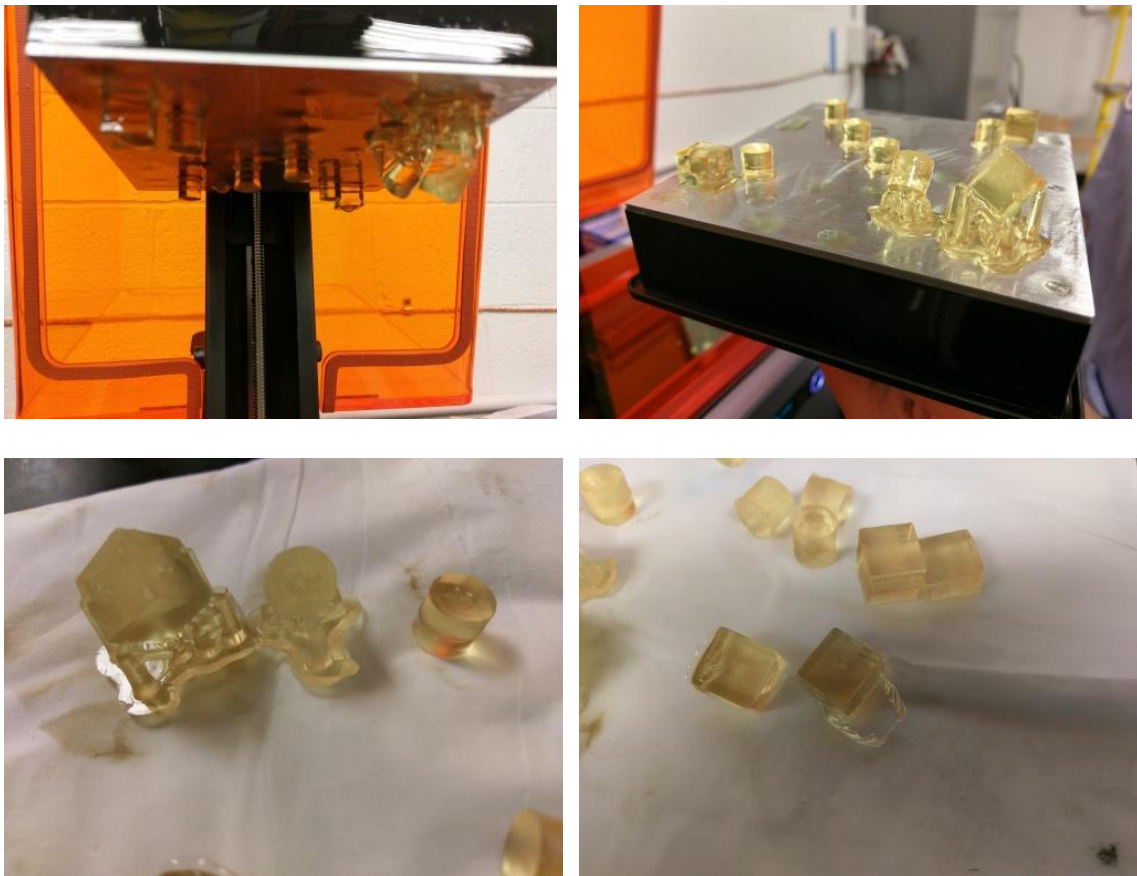

Figure 5.1 Images of DB-1 after being introduced to the Formlabs 1+ (polymerized).

According to FormLabs Help and Support, the resin partially cures in the silicone layer at the bottom of the tank and they recommended changing the tanks for every two liters of resin used. It would be interesting to know the source of silicone they use, as it may be possible that the hydrophobicity of organosilicones could prevent adhesion between the resin and the tank if a more hydrophilic resin with higher surface tension values was selected. Also to note, many vendors of photocurable resins share information on how well a resin adheres to substrates; so it was believed to avoid monomers/oligomers that have enhanced adhesion properties and this would be a requirement when trying to introduce foreign resins into their SLA tanks. Additional testing with polyethylene glycol (PEG) diacrylates (monomer with hydrophilicity) and low PI concentrations (0.1 wt. %) of BAPO did not adhere strongly to the organosilicone layer upon irradiation with the Phoseon lamp.
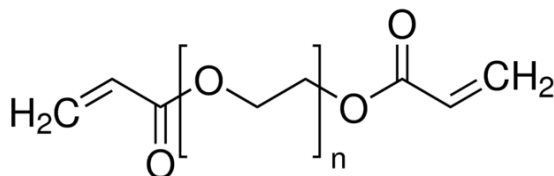

Figure 5.2 PEG diacrylates. Their ethylene oxide groups can be water soluble depending on their molecular weight.

5.2 Dynamic Mechanical Analysis (DMA)

The DMA's ability to give modulus values for each point in a temperature scan has proven to be a valuable tool for formulating polymers and polymers loaded with filler (inert or propellant) by providing key information about polymer network structure and the degree of cure. For this application, DMA provided information relating to cure depth limitations, critical solids loading, Ultimate Tg and Tg related phenomena, and how introducing solids can affect storage modulus (E') and loss modulus (E''). The DMA data for the samples,

investigated in this work (listed in Table 4.3), is given in Figures 5.3, 5.4, 5.5, and Figure

5.6. Some data is not reported due to sample breakage either prior to or during testing.
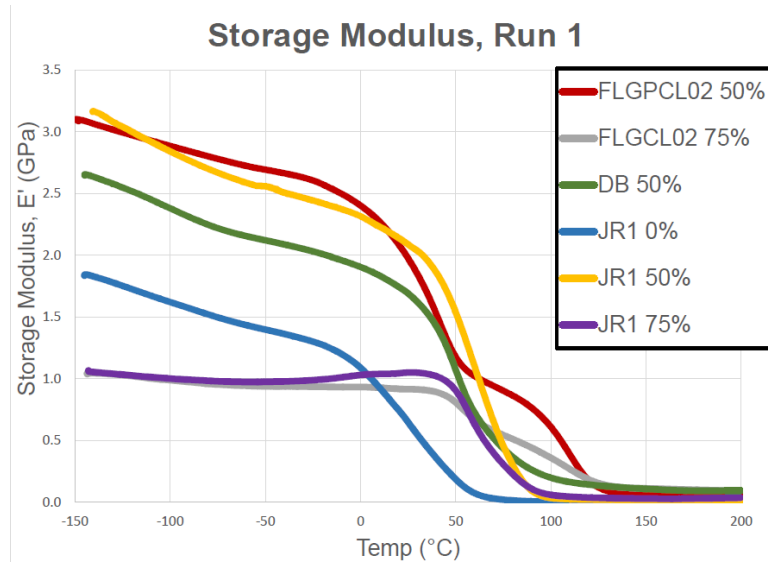

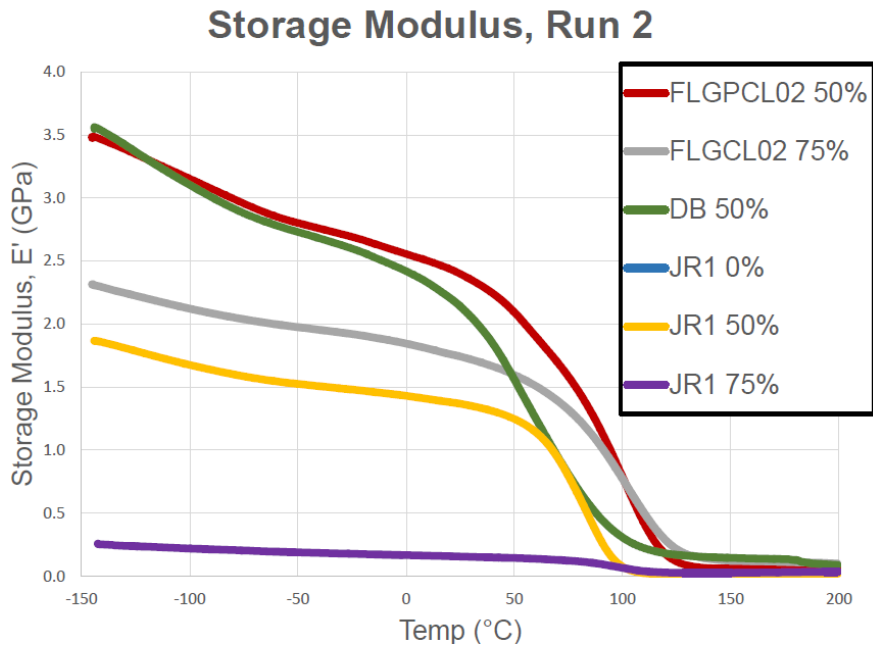**Figure 5.3** Storage modulus (E') of UV cured formulations from Table 4.3 (1st Run) obtained by DMA.

Figure 5.4 Storage modulus (E') of UV cured formulations from Table 4.3 (2nd Run) obtained by DMA.

Table 5.1 Ultimate T_g Values Identified as the Peak of the E" Curve

Mix	Tg (°C)
1 - FLGPCL02, 50 wt% melamine	101.53
2 - FLGPCL02, 75 wt% melamine	104.16
3 - DB1, 50 wt% melamine	60.62
6 - JR1, 0 wt% melamine	Broken sample
7 - JR1, 50 wt% melamine	84.59
8 - JR1, 75 wt% melamine	100.50

In typical DMA experiments for thermosetting polymers, a sample is tested twice to ascertain any changes in the polymer network structure after heating. A shift in glass transition temperature (Tg) between the first and second runs often indicates that the polymer was not fully cured and required post-curing to ensure full extent of conversion or reaction. In Figures 5.7 and 5.8, a normalized loss modulus is plotted to compare the Tg between the first and second runs of the JR1 formulation and FLGPCL02 commercial formulation with different filler loadings. For the 50 wt. % and 75 wt. % JR1 formulations, the Tg increased between the first and second run, thereby indicating a reduction in the extent of cure during photo-polymerization. Without second run data for the unfilled JR1 formulation, it is difficult to attribute this trend to the lack of penetration depth of the UV (too thick of samples) or whether the melamine is affecting the generation of free radicals and their mobility during cure. There is also the possibility of partially solubilized particles and aggregation of solids contributing to the lack of penetration depth as Ostwald ripening would have an adverse effect on curing. Future experiments will be conducted to isolate

the effect of UV penetration depth and its influence on cure. When comparing the 50 wt. %
and 75 wt. % JR1 formulations, the Tg increased more with higher filler loading between
the first and second runs. Also, the ultimate Tg of the second run is higher with more filler.
With more filler present, the polymer chains become restricted from the segmental motion
that occurs during the glass to rubber transition and results in a higher Tg. Because the Tg
of the first runs of the 50 and 75 wt. % samples were similar and the change in Tg was
more significant for the 75 wt. % formulation, we speculate that the presence of melamine
influences the extent of cure and that there may be a threshold value for filler content as
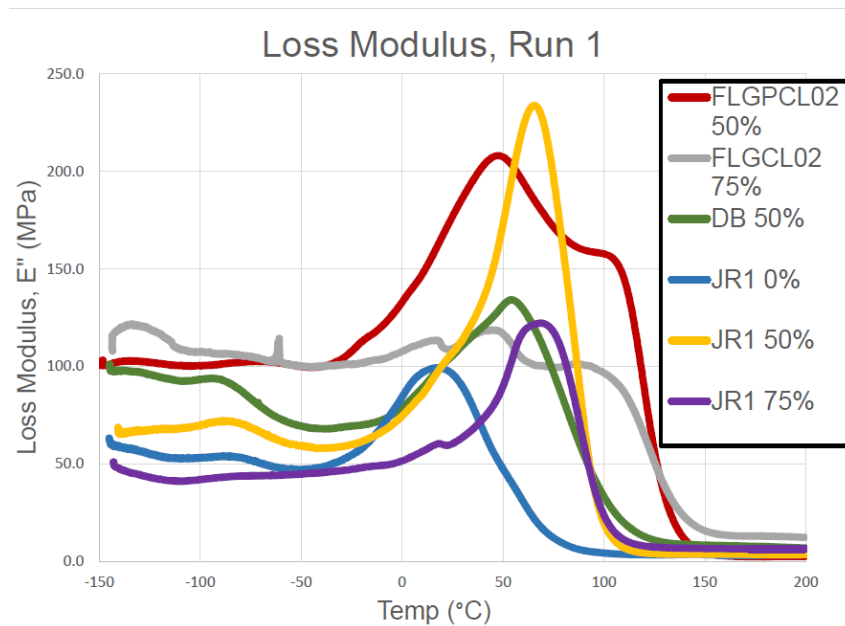observed in the literature [17].

Figure 5.5 Loss modulus (E") of UV cured formulations from Table 4.3 (1st Run) obtained
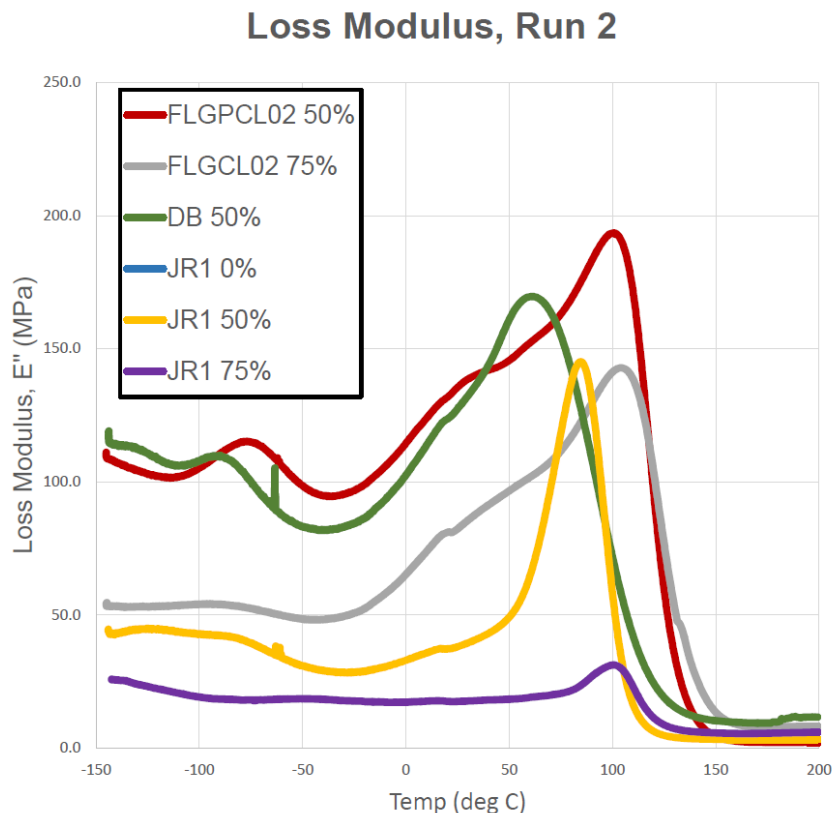by DMA.

Figure 5.6 Loss modulus (E'') of UV cured formulations from Table 4.3 (2nd Run) obtained by DMA.

In Figure 5.7, the loss modulus is shown for the first and second DMA scans for the FLGPCL02 formulations with 50 and 75 wt. % melamine. In the first DMA scan for both formulations, multiple peaks appear in the loss modulus data and suggests the formation of alternate network structures. This is an indication that homopolymerization kinetics dominate the copolymerization kinetics that ties each material into the polymer network structure. Because the sample cure was quenched due to diffusion limitations of the free radicals, we had the ability to observe how the polymer structure was formed and how it was influenced by the amount of filler. The fact that the ultimate Tg remained unaffected (as observed in the second DMA scans) does not signify a negative impact of the melamine on the mechancial/thermal properties of the polymer. However, it is important to consider that the filler has the potential to influence the formation of polymer

46

network structure and properties. For example, the 75 wt. % melamine formulation induced the formation of an additional network structure compared to the 50 wt. % formulation, thereby showing that melamine content influenced the formation of the polymer network structure. The ability to use DMA to investigate the polymer network structure will assist in selecting monomers to blend into the formulation in future work. For example, the JR1 formulations shown in Figure 5.7 do not show the presence of alternate network structure and suggests that isobornyl acrylate copolymerizes readily with the urethane acrylate monomers.
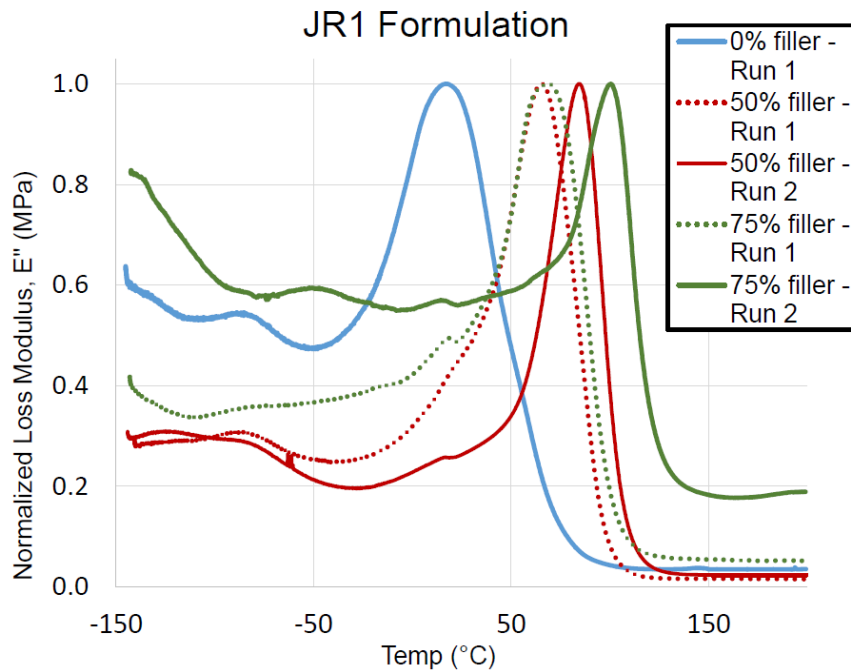

Figure 5.7. Loss modulus (E″) data for 1st and 2nd runs from DMA scans for JR1. These plots compare the effect of melamine content on the Tg of the JR1 Formulations and how the polymer network structure changes after heating.
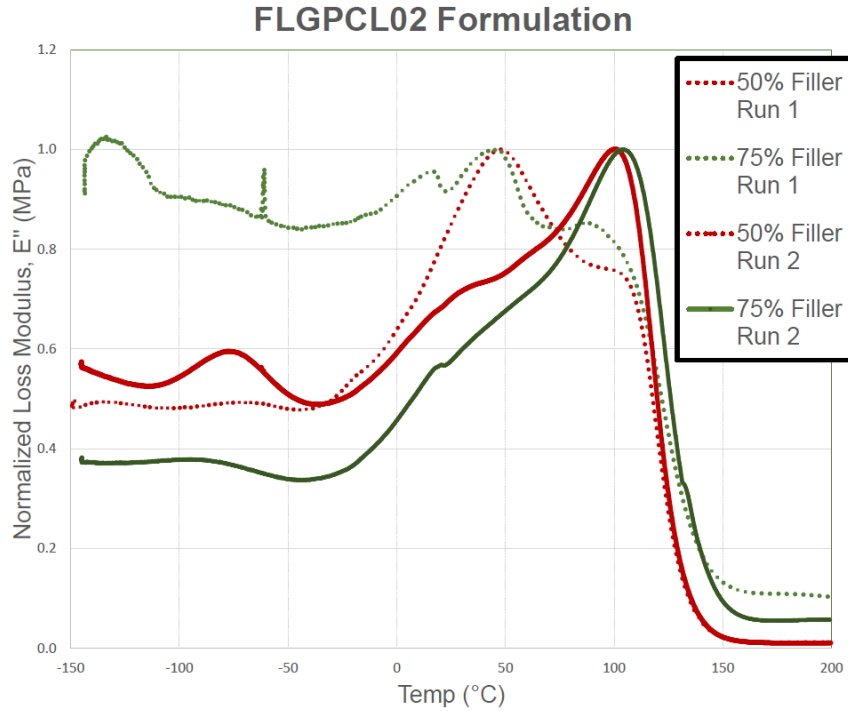
Figure 5.8 Loss modulus (E'') data for 1st and 2nd runs from DMA scans for FLGPCL02. These plots compare the effect of melamine content on the Tg and network formation of the FLGPCL02 formulations.

5.3 Tensile Testing

Tensile testing for composite materials has proven to be a valuable tool for formulating polymer composites as the results from this technique can be very useful for downselecting formulation ingredients and it gives predictions on polymer behavior under stress [22]. In this set of experiments, the effects of filler at varying concentrations was evident in the experimental runs, and the profile of the stress/strain curves generally correpsond to trends and observations in the literature [23, 24]. Increasing the concentration of melamine powder (considered an organic rigid filler) raised the modulus corresponding to the increase in concentration as depicted in Figure 5.9. Due to the brittle nature of these composites, some data is not reported due to sample breakage.
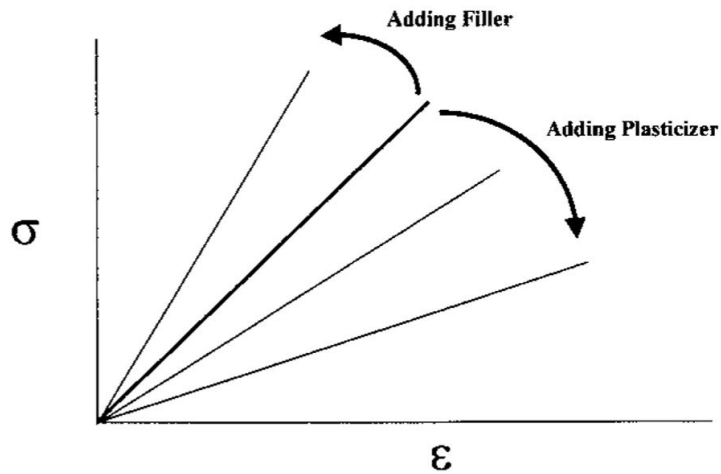
Figure 5.9 Typical stress-strain curves outlining the effects of polymer formulating.

Source: Menard, Kevin P. Dynamic Mechanical Analysis: A Practical Introduction. Boca Raton: CRC Press, 1999

Agglomeration was difficult to recognize, when the suspensions were prepared, due to turbidity within the samples, but it became evident once the samples cured (see Figure 5.10). This could be contributed to insufficient mixing, Ostwald Ripening and/or the settling of larger particles (d(0.9) melamine – 174.09µm). This puts emphasis on why a Flackek should be used for efficient mixing, or why the ceramic industry utilizes ball mills to deagglomerate/reduce particle size and employ dispersants for preventing agglomeration in suspension. Also, the scattering of light within the suspension and the resulting degree of cure would play a tremendous role in how well the monomer polymerized around the wetted solids to form a polymer binder. Sample inhomogeneity has widely been cited as a problem in literature [23, 24, 25] and results correlate with propellant researchers who have investigated the failure mechanism of hydroxyl terminated poly-butadiene (HTPB) binder systems filled with ammonium perchlorate (AP) and aluminum (Al). van Ramshorst [23] frequently cited inhomogeneity within the

samples, in which the data was very scattered due to the large particle size of AP (ca. 200 μm).

Stress as a function of strain plots for the specimens in this study are shown in Figure 5.11. A strain rate of 5mm min^{-1} at 25°C was implemented. The pneumatic gripping clamps of the Instron were sufficiently powerful enough to damage many of the solid impregnated (brittle) samples. For such reasons, limited replicates were able to be tested. This phenomenon was reported by Wang et al. [24] who were able to incorporate an aluminum gripping jaw which was capable of avoiding initial pre-strain on the sample before testing had begun. Table 5.2 highlights the mechanical properties that were calculated based on the stress-strain diagrams for the formulations in Figure 5.11. A linear plot was constructed to easily observe the affect of solids loading on modulus and ultimate strength in Figure 5.12. The trends followed the literature for samples with solids loadings of 0 wt./wt. % through 40 wt./wt.% as the slope of the curves increased and shifted to the left as depicted in Figure 5.9 and Figure 5.12 [13, 27]. Also, the point of fracture followed the same trend as the modulus increased but decreased ultimate strength. Importantly, the data iterates that there is a clear issue with solids loading and tensile strength for this resin blend with 50 wt./wt. % melamine as the samples were too brittle to even clamp into the Instron. In-situ SEM images of the fracture surface, taken by van Ramshorst [23], confirmed that large AP particles separated from the binder; hence, there was little attraction between the large AP particles and the polymer binder. Similarly, it is believed that little attraction between the DB polymer and the large melamine particles enabled a clean separation between binder and suspended particle (see Figure 5.13). Tensile testing performed by van Ramshort [23] made use of crosshead speeds of 750 μm min^{-1}, which is considerably slower than the strain rates incorporated for this study; however, both studies

are examining failure mechanisms based on void formation, particle size affects and sample inhomogeneity with similar outcomes. Efforts involving in-situ SEM with tensile testing would be highly advantageous in examining polymer mechanical deformation processes.

Wang et al. [24] investigated a similar binder system for propellant as van Ramshort [23], but quotes differing distributions on the particle sizes of AP. This was to increase AP solids loading to as high as almost 70.0 wt./wt. % AP (9.5 wt./wt. % small, 60.0 wt./wt. % larger). These samples were tested uniaxially with varied temperature (233, 243, 253 and 298 K) and constant crosshead rates (28, 280, 1000 and 3000 mm s^{-1}). The variations of mechanical parameters tested at different temperatures were similar to those tested in this study with different solid particle concentrations. Wang [24] reported that (E – the elastic modulus or Young's Modulus) increased with decreasing temperature, comparable with the trend of E increasing with increasing solids loading or E decreasing with the addition of plasticizer (see Figure 5.9). This is explained by the mobility of polymer chains and their respective movement with increasing/decreasing temperature or restriction by introducing filler. This has been extensively researched and has been monitored by DMA in this study and in the literature [21]. The eventual mechanical failure mechanism is put down to microcrack initiation due to stress concentrations arising from testing. This phenomena is associated with dewetting, or pulling the binder off of filler particles with uniaxial tensile testing. This was observed and characterized via SEM (see Figure 5.13) for the DB resins. The appearance of cavities and bare melamine particles are apparent and consistent with the literature as increasing filler leaves less volume of binder to hold the matrix together. Wang et al. [24] reported similar fracture of propellant samples as HTPB binder would actually tear from the added stress and SEM confirmed holes where dewetted AP particles used to be.

From Figure 5.12 (linear curve) and Table 5.2, it could be observed that the DB resin with solid particles was becoming stiffer as the solids loading increased. This was evident as the E values increased, while ε_{max} decreased with increasing filler concentration. This coincides with literature [23, 24] and what the DMA data reported previously. The polymer chains were becoming more restricted with increasing solids loading. Decreasing the temperature (as observed by Wang et al [24]), or increasing the solids loading (as observed in this study) has been observed to increase the stiffness, hence E increases as does ε_{max} (see Figure 5.12 and Table 5.2). Figure 5.10 depicts the 40 wt./wt.% solids loaded sample in DB polymer binder undergoing tensile testing. The sample had started to reach its critical solids loading limit and was becoming very brittle. The E value had increased from 73 MPa for the 30 wt./wt.% to 80 MPa for 40 wt./wt.%.
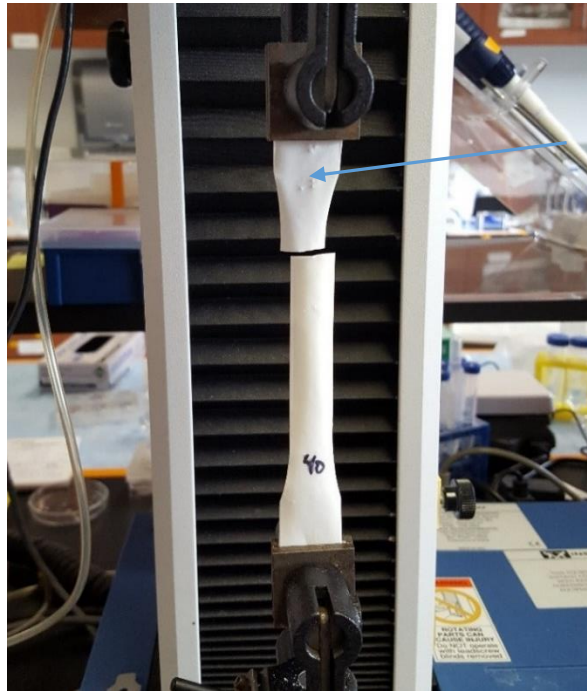

Figure 5.10 Tensile testing of DB with 40 wt./wt. % melamine. The agglomeration within the suspension became obvious once the formulation was UV cured. Agglomerated particles arising from inhomogeneity in suspension. Attributed to insufficient mixing/deagglomeration.

Table 5.2 Mechanical Properties of Formulations Tested for Tensile Testing

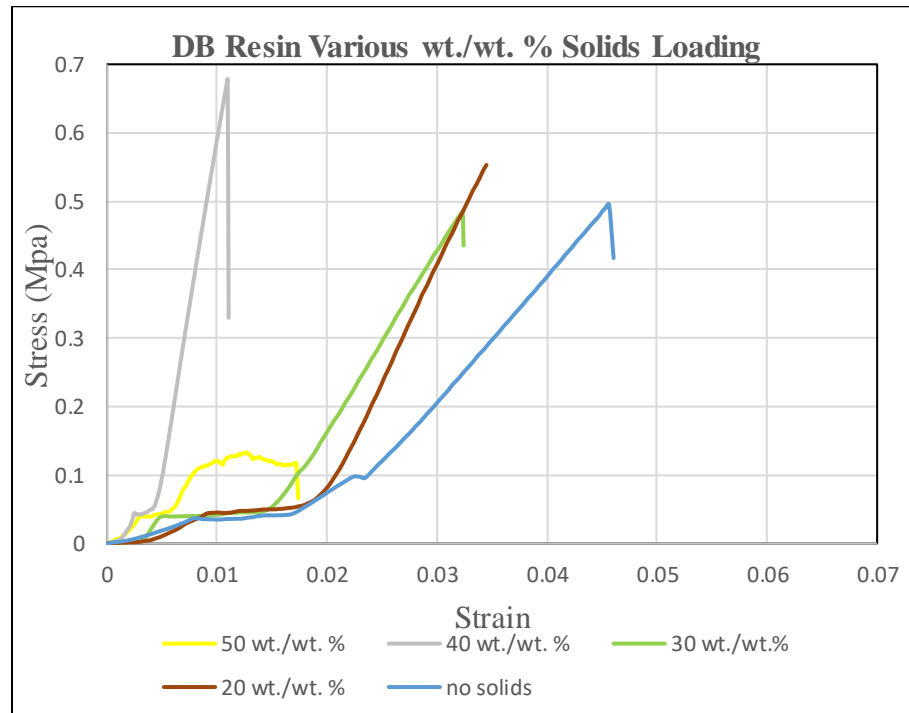| Sample	Maximum Load (N)	σ_{max} (MPa)	ε_{max}	Modulus (MPa)	Notes
DB (no solids)	105	0.49	0.04	227.48	
DB (20 wt.% solids)	72	0.48	0.032	465.27	Brittle
DB (30 wt.% solids)	73	0.55	0.034	517.41	Brittle
DB (40 wt.% solids)	80	0.67	0.01	878.37	Brittle
DB (50 wt.% solids)	15	0.13	0.01	260.36	Highly brittle sample. Limit reached on solids loading for this resin

Figure 5.11 Stress-strain curves for the DB polymer suspensions. Modulus values increase as well as ε_{max} coinciding with literature reports
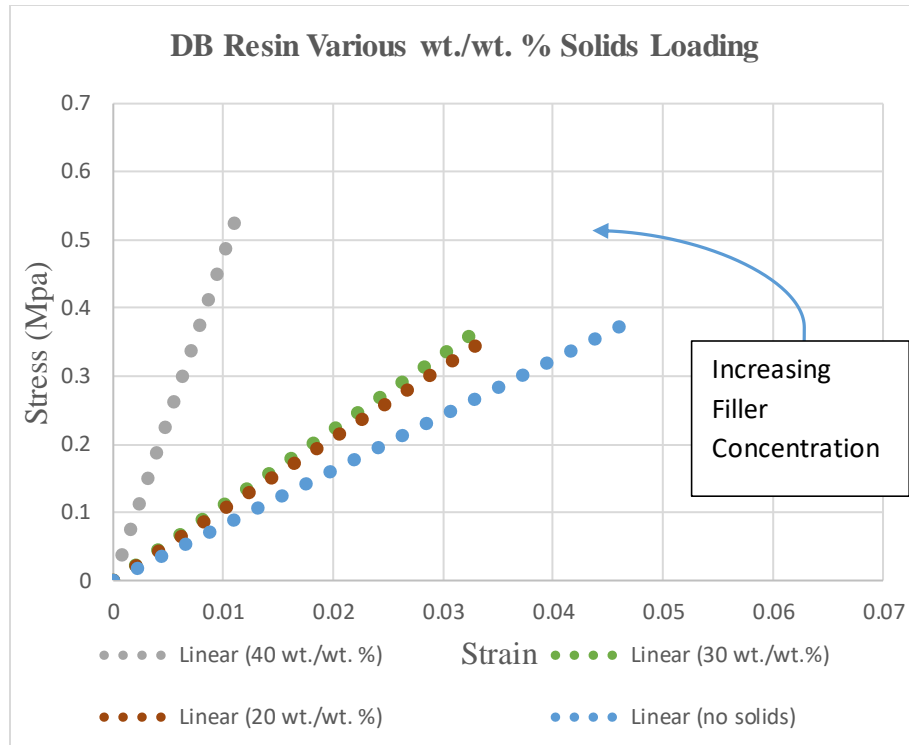
Figure 5.12 Linear plots of the stress strain curves for the DB suspensions. Loading filler into the polymer followed trends reported in Menard (Figure 5.9)

Tian and Yu [26] investigated UV-cured epoxy composites loaded with solid polymer microspheres prepared by sol gel dispersion polymerization at varying concentrations. Interestingly, their composite materials follow opposite trends exemplified by this work indicating modulus decreases with increasing weight fraction of solids in the composite. This indicates that the composition of the solid filler within a polymer composite needs be thoroughly understood as well as the resulting mechanical properties when stress is added. Work carried out by Fernandes and Kirwan et al. [27] investigated composite blends of purified epoxidized waste vegetable (EVO) and diglycidyl ether bisphenol-A (DEGBA) to locate alternative/renewable sources for epoxy resins. The composites consisted of milled recycled carbon fiber (MCF) reinforcements with content loads as high as 30 wt. %. Tensile testing on the respective formulations coincided with what was observed in this study as increasing organic filler content increased the values of Young's Modulus in both instances.
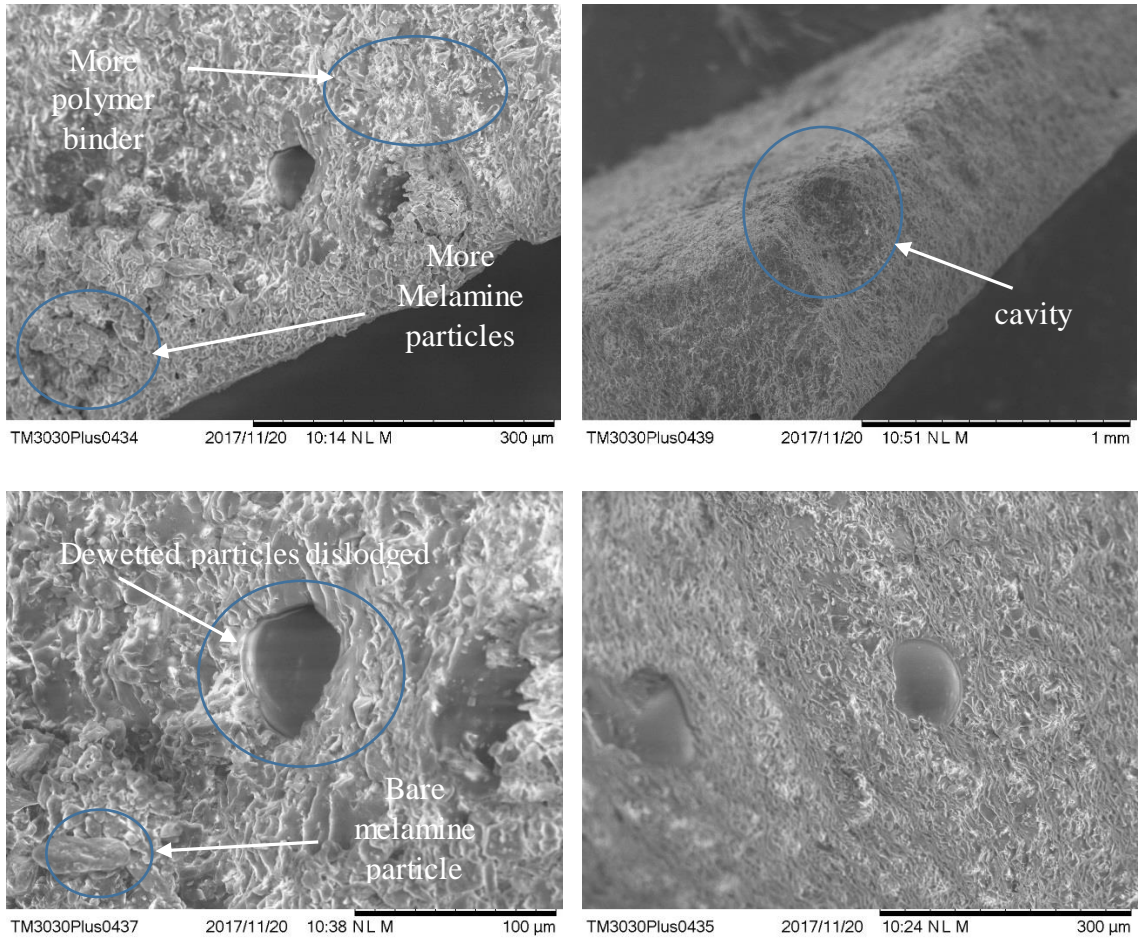
Figure 5.13 SEM images of DB resin with 40 wt./wt.% melamine. The observance of microcracks and fractured melamine particles. Microcracks, fractures and inhomogeneity were all present and led to fracture. The dewetting of particles is apparent as the circular holes are where larger melamine particles once resided.
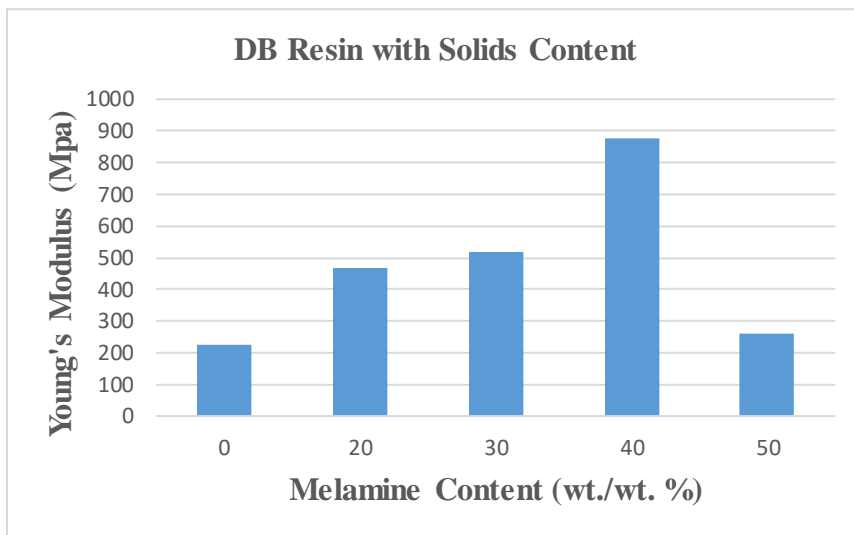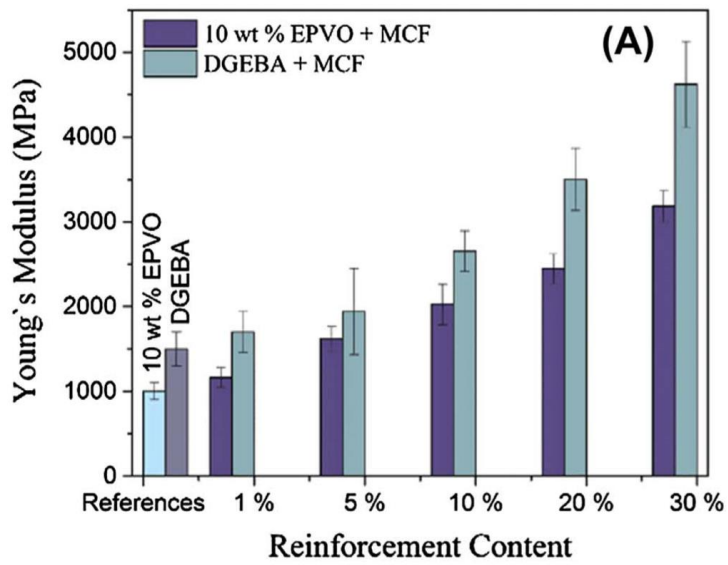
Figure 5.14 Trends observed with DB polymer composite modulus values. DB composite Modulus (bottom) coincide with those reported in the literature as epoxy polymer composites with MCF Modulus values (top) increased with increasing filler concentration. The decrease in Modulus for DB at 50 wt./wt. % melamine indicated that the critical solids loading for this sample had been achieved.

Source: Fernandes, Felipe C.; Kirwan, Kerry; Lehane, Danielle; Coles, Stuart R. "Epoxy resin blends and composites from waste vegetable oil." European Polymer Journal, 89, (2017): 449-460.

Landsem and Jensen et al. [28] investigated altering the polymer matrix and the

respective mechanical properties of a polymer composite formulation when subjected to

tensile testing. The formulations consisted of 60 wt./wt. % HMX as solid filler, with glycidyl azide polmer (GAP) and an isocyanate and/or alkyne at differing ratios for the curing agent. Tensile testing (tensile strength, elastic modulus and elongation at break) was evaluated based on historical/legacy formulations to give a rough indication of what polymer system to incorporate and what mechanical properties to strive for, while DMA was utilized to identify the Tg, investigate interactions between binder and filler and characterize ways for mechanical improvements. Tensile tests revealed GAP with alkyne curing agent and the addition of plasticizer was able to deliver the desired mechanical properties, which could lead to the belief that plasticizer is necessary to balance or "tune" the resulting mechanical properties based on the difficulties of homogeneously impregnating polymer with solids and issues involving solubility of filler in binder systems.

CHAPTER 6

SUMMARY AND CONCLUSIONS

With the foundations of Additive Manufacturing (AM) already set and ample examples from industry, the military's willingness and desire to investigate innovative technologies to print complex geometries focuses on SLA techniques that hold the potential to deliver the next generation of propulsion charges and achieve some of the past works to increase gun performance[1]. Formulating with inert acrylates and solids to gain understanding on how to formulate acrylates with solids suspended within appears to be a beneficial way to aid the propulsion formulators on some of the challenges and obstacles ahead. Formulating an energetic or non-energetic suspension to be added to an SLA tank introduces many challenges for the formulator including abnormal and unwanted rheological behavior, undesired mechanical properties, settling of the dispersed solid, partial solubility of the solid in the resin, Ostwald ripening, and poor curing from photopolymerization. This research shows some of the initial efforts to formulate new polymeric binders for SLA resins. The ability to print custom resins in an SLA printer has been established. DMA has proved to be a valuable tool in observing how changes in the formulation (monomers, PI content, filler content, etc.) influences Tg and the formation of the polymer network structure. Tensile testing can validate and is a good accomplice to DMA data for information regarding the structural integrity of polymer composite formulations.

6.1 FUTURE WORK

Formulation development and considering stabilizing the monomer/oligomer suspensions will be valuable for maintaining homogeneity within the SLA tank and for the subsequent

polymer formed. DMA provides a quick determination of polymer network structure and mechanical/thermal properties and should be used for down-selection. Tensile testing is important for determining the behaviors of the polymers and qualifying composite formulations at the interface between polymer binder and suspended particle(s). Future tensile tests should include varied strain rates, temperatures and environmental conditions for further analysis of polymer composites and the structural integrity. Also, high rate compression testing will be used in conjunction with flexural and fracture properties to fully characterize the mechanical properties of newly formulated SLA materials. To qualify formulations, the mechanical property data generated will be compared to baseline formulations that are known to be good performers. AM allows for printing new SLA propellant formulations into a host of geometries, thereby enabling the assessment of mechanical properties that are traditionally difficult to obtain for propellant formulations.

TIME-TEMPERATURE SUPERPOSITION THEORY

Strain is a function of temperature. This is shown in Figure A.1. This relates to the study of Lei and Frazier [29] by portraying strain to be accelerated by faster heating ramps.
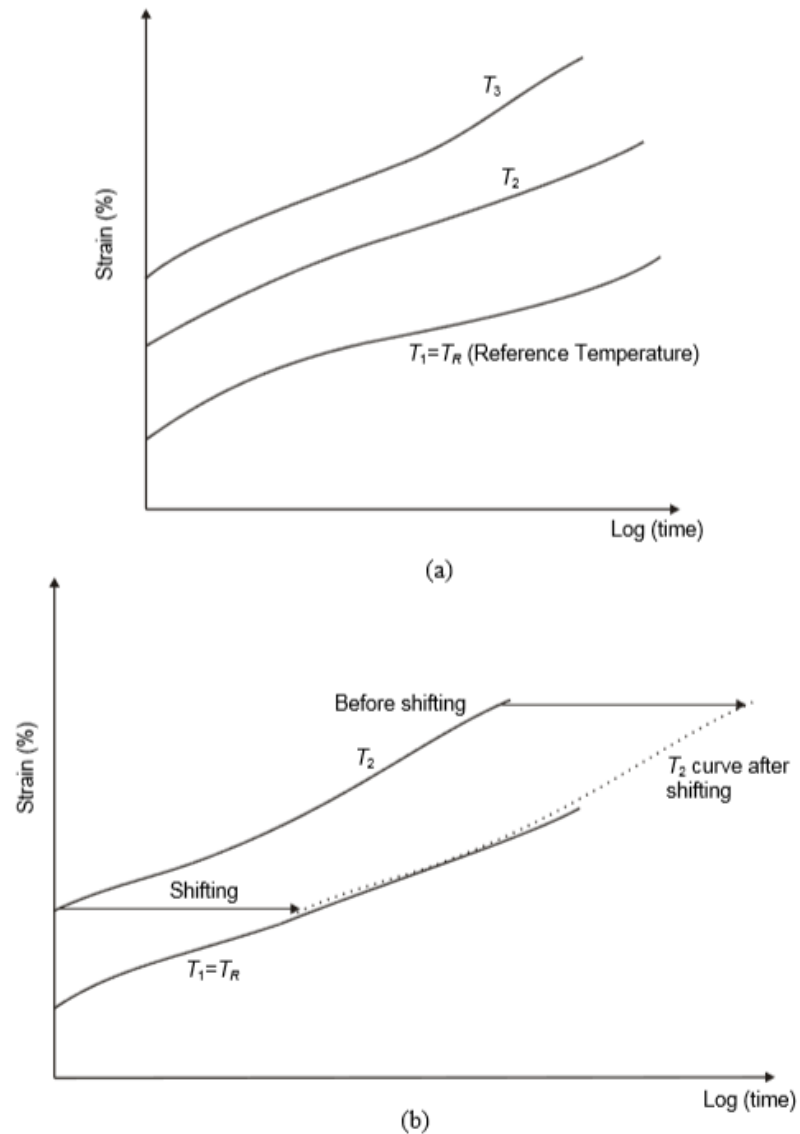

Figure A1 Idealized strain curves (a) and the respective shift with differing temperatures.

Source: Alwis, K. G. N. C.; Burgoyne, C.J. "Time-Temperature Superposition to Determine the Stress-Rupture of Aramid Fibres." Applied Composite Materials, 13, 4 (2006) 249-264.

REFERENCES

1. Yagci, Yusuf; Jockusch, Steffen; and Turro, Nicholas J., "Photoinitiated Polymerization: Advances, Challenges and Opportunities," *Macromolecules*, 43 (2010): 6245-6260.

2. DeSimone, Joseph M.; Ermoshkin, Alexander; Ermoshkin, Nikita, Samulski, Edaward T. "Continuous Liquid Interphase Printing." Redwood City, CA (US), 2016.

3. Department of Defense, Interior Ballistics of Co-Layered Gun Propellant.

4. Department of Defense, Next Generation Propulsion Charges for Guns.

5. Fisher, Michael. "In Situ Manufacturing of Polymer Nanocomposites for Energetic Applications." *DSIAC Journal* 4, 1 (2017). 4-10.

6. Jeromin, Julia and Ritter, Helmut, "Cyclodextrins in Polymer Synthesis: Free Radical Polymerization of a N-Methacryloyl-11-aminoundecanoic Acid/β-Cyclodextrin Pseudorotaxane in an Aqueous Medium" *Macromolecules*, 1999, *32* (16), pp 5236–5239.

7. Alupei, I.C.; Alupei, V.; Ritter, H. "Photoinitiated polymerization of β-cyclodextrin/methyl methacrylate host/guest complex in the presence of water soluble photoinitiator, thioxanthone-catechol-O,O′-diacetic acid," *Journal of Inclusion Phenomena and Macrocylic Chemistry*. 68, 1-2 (2010): 147-153.

8. Fouassier, Jean-Pierre; Morlet-Savary, Fabrice; Lalevée, Jacques; Allonas, Xavier and Ley, Christian. "Dyes as Photoinitiators or photosensitizers of polymerization Reactions." *Materials*, 3 (2010): 5130-5142.

9. Miao, Shida; Wang, Ping; Su, Zhiguo; and Zhang Songping. "Vegetable-oil-based polymers as future polymeric biomaterials." *Acta Biomaterialia*, 10, 4 (2014): 1692-1704.

10. Marie, Jérémy; Bourret, Julie; Geffroy, Pierre-Marie; Smith, Agnés, Smith; Chaleix, Vincent; Chartier, Thierry. "Eco-friendly alumina suspensions for tape-casting process," *Journal of the European Ceramic Society*, 37, 16 (2017): 5239-5248.

11. Lu, Jue and Wool, Richard P. "New sheet molding compound resins from soybean oil. I. *Synthesis and Characterization*." 46, 1 (2005): 71-80.

12. Liu, Ren; Luo, Jing; Ariyasivam, Sharonie; Liu, Xiaoya; Chen, Zhigang. "High biocontent natural plant oil based UV-curable branched oligomers." Progress in Organic Coatings, 105 (2017): 143-148.

13. Chartier, T.; Badev, A.; Abouliatim, Y.; Lebaudy, P.; Lecamp, L. "Stereolithography process: Influence of the rheology of silica suspensions and of the medium on polymerization kinetics – Cured depth and width", *Journal of the European Ceramic Society*, 32 (2012): 1625-1634.

14. Fouassier, Jean-Pierre; Morlet-Savary, Fabrice; Laleveé, Jacques; Allonas, Xavier; Ley, Christian. "Dyes as Photoinitiators or Photosensitizers of Polymerization Reactions," *Materials*, 3 (2010): 5130-5142.

15. Sitzmann, E. V. Critical Photointiators for UV-LED Curing: Enabling 3D Printing, Inks and Coartings." Radtech, Redondo Beach, CA, March 2015.

16. Painter, Paul C. and Coleman, Michael M. *Essentials of Polymer Science and Engineering*. Lancaster: DES*tech* Publications, 2009.

17. Menard, Kevin P. *Dynamic Mechanical Analysis: A Practical Introduction*. Boca Raton: CRC Press, 1999.

18. Office of Naval Research, Ultraviolet Curing of Highly Loaded Ceramic Suspensions for Stereolithography of Ceramics.

19. Chartier, Thierry; Dupas, Cyrielle; Geffroy, Pierre-Marie, Geffroy; Pateloup, Vincent; Colas, Maggy; Cornette, Julie; Guillemet-Fritsch, Sophie. "Influence of irradiation parameters on the polymerization of ceramic reactive suspensions for stereolithography," *Journal of the European Ceramic Society*, 37, 15 (2017): 4431-4436.

20. Badev, A.; Abouliatim, Y., Chartier, T.; Lecamp, L.; Lebaudy, P.; Chaput, C.; Delage, C. "Photopolymerization kinetics of a polyether acrylate in the presence of ceramic fillers used in stereolithography," Journal of *Photochemistry and Photobiology A: Chemistry*, 222, 1 (2011): 117-122.

21. Lei, Hong; and Frazier, Charles E. "A dynamic mechanical analysis method for predicting curing behavior of phenol-formaldehyde resin adhesive," *Journal of Adhesion Science and Technology*, 29 (10) 2015: 981-990.

22. Courtney, Thomas H. *Mechanical Behavior of Materials 2nd Edition*. Long Grove: Waveland Press, 2005.

23. Van Ramshorst, Marthinus C. J.; Di Benedetto, Giuseppe L.; Duvalois, Willem; Hooijmeijer, Peter A.; van der Heijden. "Investigation of the Failure Mechanism of HTPB/AP/Al Propellant by In-situ Uniaxial Tensile Experimentation in SEM." *Propellants, Explosives, Pyrotechnics*, 41, 4 (2016): 700-708.

24. Wang, Zhejun; Qiang, Hongfu; Wang, G. "Experimental Investigation on High Strain Rate Tensile Behaviors of HTPB Propellant at Low Temperatures." *Propellants, Explosives, Pyrotechnics*, 46, 6 (2015): 814-820.

25. Silverman, Edward M. "Material Properties of Chopped Glass-Fiber/Polyester Sheet Molding Compound." Paper presented at the 37th Annual Conference,

Reinforced Plastics/Composites Institute, The Society of the Plastics Industry, Inc., January 11-15, 1982.

26. Tian, Qiong and Yu, Demei. "Preparation and properties of polymer microspheres filled epoxy composite films by UV-curable polymerization." *Materials and Design*, 107, 5 (2016): 221-229.

27. Fernandes, Felipe C.; Kirwan, Kerry; Lehane, Danielle; Coles, Stuart R. "Epoxy resin blends and composites from waste vegetable oil." *European Polymer Journal*, 89, (2017): 449-460.

28. Landsem, Eva; Jensen, Tomas L., Kristensen, Tor E., Hansen, Finn K.; Benneche, Tore; Unneberg, Eril. "Isocyanate-Free and Dual Curing of Smokeless Composite Rocket Propellants." *Propellants, Explosives and Pyroyechnics*, 38 (2013): 75-86.

29. Alwis, K. G. N. C.; Burgoyne, C .J. "Time-Temperature Superposition to Determine the Stress-Rupture of Aramid Fibres." *Applied Composite Materials*, 13, 4 (2006) 249-264.